TauSpinner ALGORITHMS FOR INCLUDING SPIN AND NEW PHYSICS EFFECTS IN $\bar{q}q \to Z/\gamma^* \to \tau\tau$ PROCESS

A.Yu. Korchin [a,b,c], E. Richter-Was [c], Z. Was [d]

[a]NSC Kharkiv Institute of Physics and Technology, 61108 Kharkiv, Ukraine
[b]V.N. Karazin Kharkiv National University, 61022 Kharkiv, Ukraine
[c]M. Smoluchowski Institute of Physics, Jagiellonian University
Łojasiewicza 11, 30-348 Kraków, Poland
[d]Institute of Nuclear Physics Polish Academy of Sciences
Radzikowskiego 152, 31-342 Kraków, Poland

Received 7 January 2026, accepted 5 February 2026, published online 16 March 2026

The possible anomalous New Physics contributions to dipole and weak dipole moments of the τ lepton bring renewed interest in development and revisiting charge-parity violating signatures in τ-pair production in Z-boson decay at energies of the LHC. In this paper, we discuss effects of anomalous contributions to polarisation and spin correlations in the $\bar{q}q \to \tau^+\tau^-$ production processes, with τ decays included. Due to the complex nature of the resulting distributions, Monte Carlo techniques are useful, in particular for event reweighing with studied New Physics phenomena. Extensions of the Standard Model spin amplitudes, within the Improved Born Approximation used for the matrix element, are implemented in the TauSpinner program. This is mainly with τ dipole and weak dipole moments in mind, but is applicable to arbitrary New Physics interactions, provided they can be encapsulated into the Standard Model $2 \to 2$ structure of matrix element extensions. The implementation allows one also to introduce an arbitrary phase-shift between vector and axial-vector couplings of Z boson to τ leptons, which would have impact on the observed transverse spin correlations. Basic formulas and algorithm principles are presented, together with distributions for the spin-correlation matrix. Numerical examples of impact on experimental signatures are shown in the case of $\tau^\pm \to \rho^\pm\nu_\tau \to \pi^\pm\pi^0\nu_\tau$ decays. Information on how to use and configure the TauSpinner program is given in Appendix B.

DOI:10.5506/APhysPolB.57.3-A3

1. Introduction

The possible anomalous New Physics contributions to dipole and weak dipole moments of the τ lepton bring renewed interest in development and revisiting charge-parity (CP) violating signatures in the τ-pair production in Z-boson decay at the LHC energies. Such a process has been studied in the pp collisions at the CERN LHC experiments in a wide range of invariant

masses of the outgoing τ-lepton pair [1–3]. What was not explored so far is the precise measurement of the transverse spin correlations of the outgoing pair of τ leptons.

The TauSpinner program [4, 5] is a convenient tool to study observables sensitive to the New Physics (NP) effects in hadron colliders. It allows one to include NP and spin effects in case they are absent in event samples generated with general purpose MC generators such as PYTHIA [6] or Sherpa [7]. Program development has a long history driven by the expanding scope of its initially designed applications [4]. First, the longitudinal spin effects in the case of the Drell–Yan (Z, W) and the Higgs-decay processes of τ leptons at the LHC [4] were implemented. Later, it was extended to applications for the NP interactions in the hard processes, in which lepton pairs are accompanied by one or two hard jets [8], and to the transverse spin effects [9]. The implementation was then further extended, Refs. [10, 11], to allow for study of the electroweak effects and anomalous dipole moments of the τ-lepton couplings to vector bosons, Refs. [12, 13].

In recent years, anomalous dipole and weak dipole moments [14–16] of the τ-lepton interaction with γ and Z bosons gained attention when searching for NP effects, due to the indication of possible NP effects in case of the muon. In [17], we have presented an algorithm, implemented in the TauSpinner program [10], to reweight previously generated events with the NP effects added in case of the $\gamma\gamma \to \tau\tau$ hard process. These calculations include higher-order terms of dipole moments and phenomenological results. Now, we return to the $\bar{q}q \to Z/\gamma^* \to \tau\tau$ process. In the present paper, our focus is on discussing similar algorithms applied in the region around the Z-boson peak in the $\bar{q}q \to \tau\tau$ process. We evaluate numerical effects due to NP on elements of the spin-correlation matrix and show an example of experimentally accessible distributions that are sensitive to spin correlations.

We first recall, Section 2, details of formalism used to determine spin amplitudes and remind how they lead to defining the spin-correlation matrix, which, when contracted with polarimetric vectors of the τ decays, can be used for introducing spin correlations of τ-decay products. The expressions for spin amplitudes in the case of the Standard Model (SM) in the Born Approximation (BA) and NP extensions with τ-lepton dipole moments (in coupling to photon) and weak dipole moments (in coupling to Z boson) were given in [12]. Now, we complete them with explicit formulas of the Improved Born Approximation (IBA), which includes electroweak (EW) corrections as in the formalism outlined in [18]. Inspired by the measurements and publications of results of the LEP experiments [19, 20], we also introduce phase-shift between vector and axial-vector $Z\tau\tau$ couplings in the formalism of IBA, as a possible consequence of NP effects, and evaluate the impact on the amplitudes and spin correlations.

The spin correlations and spin-correlation matrix R_{ij} are first discussed in Subsection 2.1, extension of R_{ij} with the EW corrections is presented in Subsection 2.2, the phase-shift between vector and axial-vector couplings is discussed in Subsection 2.3, and some discussion on related measurements by the LEP experiments is given in Appendix A. The algorithm for event reweighting in TauSpinner is presented in Section 3. Subsection 3.1 covers issues of convention matching between the amplitudes presented in Subsection 2.2 and implementation in the TauSpinner program, and configurations with high-p_{T} jets are briefly addressed in Subsection 3.2. Numerical results for the spin-correlation matrix are given in Subsection 4.1 and the impact of NP effects on a few interesting experimental distributions is discussed in Subsection 4.2. Section 5 closes the paper. In Appendix B, we discuss technical details on how to configure the initialisation of TauSpinner with discussed NP effects in weight calculations.

2. Amplitudes and spin correlations

The formalism for calculating spin amplitude and spin correlations in the $\bar{q}q \to Z/\gamma^* \to \tau\tau$ process, as implemented in the TauSpinner algorithms, was discussed in [12, 21] for the SM and the SM extensions including dipole and weak dipole moments in the $\gamma\tau\tau$ and $Z\tau\tau$ couplings. The formalism for introducing the TauSpinner algorithms of IBA and EW corrections encapsulated into form-factors was discussed in [10]. Let us now consolidate this formalism and discuss how the existing implementations can be used to predict impact of NP effects on spin correlations in the $\bar{q}q \to Z/\gamma^* \to \tau\tau$ process. We do not define specifically what are the NP models, we just consider the effects of form-factors that they can bring:

- modification of the $\gamma\tau\tau$ vertex with the structure defined as for anomalous magnetic and/or electric form-factors;
- modification of the $Z\tau\tau$ vertex with the structure defined as for anomalous weak magnetic and/or weak electric form-factors;
- introduction of a phase-shift between vector and axial-vector couplings in the $Z\tau\tau$ vertex.

We will briefly summarise the formalism used in the following subsections.

2.1. Matrix element in $\bar{q}\,q \to Z/\gamma^* \to \tau\tau$ processes

In this subsection, details of spin correlations in the $q(k_1) + \bar{q}(k_2) \to \tau^-(p_-) + \tau^+(p_+)$ process are presented, where q stands for the u, d, s quarks. We include the s-channel exchange of the Z boson, virtual photon (γ^*), and their interference.

The $\gamma\tau\tau$ electromagnetic vertex is defined in the form

$$\Gamma^{\mu}_{\gamma}(s) = -ie\,Q_{\tau}\Big\{\gamma^{\mu}F_1(s) + \frac{\sigma^{\mu\nu}q_{\nu}}{2m_{\tau}}\left[iA(s) + B(s)\gamma_5\right]\Big\}\,, \tag{1}$$

where $e = \sqrt{4\pi\alpha}$ is the elementary charge, and α is the fine-structure constant, $Q_{\tau} = -1$, $\sigma^{\mu\nu} = \frac{i}{2}[\gamma^{\mu}, \gamma^{\nu}]$, $F_1(s)$ is the Dirac form-factor, $A(s) = F_2(s)$ is the Pauli form-factor, and $B(s) = F_3(s)$ is the electric dipole form-factor, all of which depend on $s = q^2$, where $q = k_1 + k_2 = p_- + p_+$. At the real-photon point, $F_1(0) = 1$, $A(0)$ is the anomalous magnetic dipole moment μ_{τ}, while $B(0)$ is related to the CP-violating electric dipole moment d_{τ}

$$A(0) = \frac{1}{2}(g_{\tau} - 2) = \mu_{\tau}, \qquad B(0) = \frac{2m_{\tau}}{eQ_{\tau}}d_{\tau}\,, \tag{2}$$

where g_{τ} is the gyro-magnetic factor. In (1), we choose $F_1(s) = 1$ and discuss EW radiative corrections below.

To separate the SM contribution from NP, we explicitly include the QED contribution to $A(s)$ of the first order in α [22]

$$A(s)_{\rm QED} = \frac{e^2m_{\tau}^2}{4\pi^2 s\beta}\left(\log\frac{1-\beta}{1+\beta} + i\,\pi\right). \tag{3}$$

Therefore, we have

$$A(s) = A(s)_{\rm QED} + A(s)_{\rm NP}\,, \qquad B(s) = B(s)_{\rm NP}\,. \tag{4}$$

In Eq. (4), we neglect a very small SM contribution to $B(s)$. Velocity of the τ lepton in the center-of-mass frame is denoted as $\beta = (1 - 4m_{\tau}^2/s)^{1/2}$.

The $Z\tau\tau$ vertex is defined in the form

$$\Gamma^{\mu}_{Z}(s) = -i\frac{g_Z}{2}\left\{\gamma^{\mu}(v_{\tau} - \gamma_5 a_{\tau}) + \frac{\sigma^{\mu\nu}q_{\nu}}{2m_{\tau}}\left[iX(s) + Y(s)\gamma_5\right]\right\}, \tag{5}$$

where $g_Z = e/(s_{\rm W}c_{\rm W})$, $s_{\rm W} \equiv \sin\theta_{\rm W}$, $c_{\rm W} \equiv \cos\theta_{\rm W}$, and $\theta_{\rm W}$ is the weak mixing angle. The vector and axial-vector coupling is, respectively, $v_{\tau} = T_{3\tau} - 2Q_{\tau}s_W^2$ and $a_{\tau} = T_{3\tau}$, where $T_{3\tau} = -1/2$ is the 3$^{\rm rd}$ component of the weak isospin. Further, $X(s)$ is the weak anomalous magnetic form-factor, and $Y(s)$ is the CP-violating weak electric form-factor. On the Z-boson mass shell, they are related to the weak anomalous magnetic, $\mu_{\tau}^{(w)}$, and weak electric, $d_{\tau}^{(w)}$, dipole moments, defined in the ALEPH paper [23] via

$$X\left(M_Z^2\right) = \mu_{\tau}^{(w)}(2s_{\rm W}c_{\rm W})\,, \qquad Y\left(M_Z^2\right) = d_{\tau}^{(w)}(2s_{\rm W}c_{\rm W})\,. \tag{6}$$

In the SM, $\mu_{\tau}^{(w)}$ was evaluated in Ref. [24]: $\mu_{\tau,\,\rm SM}^{(w)} = -(2.10 + i\,0.61)\times 10^{-6}$. It is therefore rather small, and this contribution is not explicitly given in our code, but can be included, if needed. The form-factors $X(s)$ and $Y(s)$ can be viewed as originating mainly from NP.

We consider the production of the polarised τ^+ and τ^- leptons, which are characterized by the polarisation three vectors in their rest frames, respectively,

$$s_j^+ = \left(s_1^+, s_2^+, s_3^+, 1\right), \qquad s_i^- = \left(s_1^-, s_2^-, s_3^-, 1\right), \tag{7}$$

where j, $i = 1, 2, 3, 4$, and the Cartesian components $\vec{s}^{\pm} = (s_1^{\pm}, s_2^{\pm}, s_3^{\pm})$ are defined with respect to the chosen reference frame[1]. For convenience, we add in (7) the 4^{th} components of the vectors, namely 1.

The matrix element squared and averaged over polarisations of the initial quarks

$$|\mathcal{M}|^2 = |\mathcal{M}_\gamma|^2 + |\mathcal{M}_Z|^2 + 2\text{Re}(\mathcal{M}_\gamma^* \mathcal{M}_Z) \tag{8}$$

determines the differential cross section

$$\frac{\text{d}\sigma}{\text{d}\Omega}\left(q\,\bar{q} \to \tau^-\tau^+\right) = \frac{\beta}{64\pi^2 s}|\mathcal{M}|^2, \tag{9}$$

where the mass of the quark is neglected.

For the polarised τ leptons, each part of Eq. (8) is expressed via polarisation vectors of τ leptons in their respective rest frames, Eqs. (7). Therefore,

$$|\mathcal{M}|^2 = \sum_{i,j=1}^{4} \left(R_{ij}^{(\gamma)} + R_{ij}^{(Z)} + R_{ij}^{(Z\gamma)}\right) s_i^- s_j^+, \tag{10}$$

where $R_{ij}^{(\gamma)}$, $R_{ij}^{(Z)}$ and $R_{ij}^{(Z\gamma)}$ are the matrices, respectively, of the γ exchange, Z-boson exchange, and $Z\gamma$ interference. In the present implementation, we include only terms linear in the form-factors $A(s), B(s), X(s)$, and $Y(s)$. The expressions for R_{ij} in BA can be found in [12].

Next, we introduce EW corrections, following Refs. [10, 18]. The amplitude in IBA, without dipole moments, can be written as

$$\begin{aligned}\mathcal{M}^{\text{IBA}} \;=\; & \frac{e^2}{s} Q_q Q_\tau \, V_{\tau q}(s,t)\, \gamma_\mu \otimes \gamma^\mu \\ & + \left(\frac{g_Z}{2}\right)^2 \frac{Z_{\tau q}(s,t)}{d(s)}\, \gamma_\mu [v_q(s,t) - a_q\gamma_5] \otimes \gamma^\mu [v_\tau(s,t) - a_\tau\gamma_5]\end{aligned} \tag{11}$$

with the shortcut notation: operator on the left of $\otimes$ is sandwiched between the spinors of the quarks, $\bar{v}(k_2)\ldots u(k_1)$, and operator on the right of $\otimes$ is sandwiched between the spinors of the τ leptons, $\bar{u}(p_-)\ldots v(p_+)$. In (11), Q_q is the charge of the quark q in units of e.

[1] The frame is such that the axis "3" is along the momentum of outgoing τ^-, the momentum of incoming quark q lies in the plane "1–3", and the axis "2" is orthogonal to the reaction plane. The following terminology is used: transverse (T) means component along axis 1, normal (N) — along axis 2, and longitudinal (L) — along axis 3.

The weak vector couplings $v_q(s,t)$ and $v_\tau(s,t)$ in IBA are complex and $(s,\,t)$-dependent

$$\begin{aligned} v_q(s,t) &= T_{3q} - 2Q_q s^2_{\rm W} K_q(s,t)\,, \\ v_\tau(s,t) &= T_{3\tau} - 2Q_\tau s^2_{\rm W} K_\tau(s,t)\,, \end{aligned} \tag{12}$$

while the axial-vector couplings are real and constant, $a_q = T_{3q}$ and $a_\tau = T_{3\tau}$. The Mandelstam variable $t = (k_1 - p_-)^2 = m_\tau^2 - s(1-\beta\cos\theta)/2$, and it reduces to $t \approx -s(1-\cos\theta)/2$ in the $m_\tau \approx 0$ limit. For more details, we refer to the original articles [10, 11] and [12].

Furthermore, $d(s) = s - M_Z^2 + is\,\Gamma_Z/M_Z$ with running Z-boson decay width, and $Z_{\tau q}(s,t)$ is the normalisation correction for the Z-boson propagator defined in Ref. [10].

For technical reasons, of an algebraic manipulation program, we cannot add EW corrections of vv_{if} to the Z exchange amplitude, because it simultaneously depends on the incoming and outgoing fermion flavours, thus cannot be absorbed into the couplings redefinition. Fortunately, as it affects vector $\times$ vector coupling only, part of the EW corrections can be moved into an effective γ-exchange amplitude (the first term in (11)). Of course, for that Z-boson (not γ) exchange correction, the photon propagator $1/s$ has to be replaced with $1/d(s)$, and the coupling e^2 with $(g_Z/2)^2$. We finally obtain the factor $V_{\tau q}(s,t)$ in (11)

$$V_{\tau q}(s,t) = \Gamma_{vp} + \left(\frac{g_Z}{e}\right)^2 s^4_{\rm W} Z_{\tau q}(s,t)\frac{s}{d(s)}\left[K_{\tau q}(s,t) - K_\tau(s,t)K_q(s,t)\right], \tag{13}$$

which include the vv_{if} contribution from Z on top of Γ_{vp}, where the normalisation correction Γ_{vp} of photon exchange includes the re-summed vacuum-polarisation loop contribution. The complex EW form-factors to vector couplings, $K_q(s,t)$, $K_\tau(s,t)$, and $K_{\tau q}(s,t)$, are defined in Ref. [10].

Equation (11) represents the improved (with EW corrections) photon exchange amplitude with running QED constant and improved Z-boson exchange, which include:

- corrections to the photon propagator coming from the vacuum-polarisation loops,
- corrections to the Z-boson propagator and couplings embedded in the form-factors $Z_{\tau q}(s,t)$, $K_q(s,t)$, $K_\tau(s,t)$, and $K_{\tau q}(s,t)$,
- contributions from the WW- and ZZ-box diagrams also included in the form-factors,
- mixed $\mathcal{O}(\alpha\alpha_{\rm s},\, \alpha\alpha_{\rm s}^2, \ldots)$ corrections originating from gluon insertions in the self-energy loop diagrams.

The EW form-factor corrections are available in the Dizet library [18] (see further details in Ref. [10]).

We can now include the dipole form-factors $A(s)$, $B(s)$, $X(s)$, and $Y(s)$ in the amplitude with EW corrections. Using Gordon identities (see details in [12]), the amplitude takes the form

$$\mathcal{M}^{\mathrm{DM}} = \frac{e^2}{s} Q_q Q_\tau \, V_{\tau q}(s,t) \, \gamma_\mu \otimes \left[A\gamma^\mu + \frac{(p_+ - p_-)^\mu}{2m_\tau}(A - iB\gamma_5) \right] + \left(\frac{g_Z}{2}\right)^2 \frac{Z_{\tau q}(s,t)}{d(s)} \, \gamma_\mu [v_q(s,t) - a_q\gamma_5] \otimes \left[X\gamma^\mu + \frac{(p_+ - p_-)^\mu}{2m_\tau}(X - iY\gamma_5) \right], \tag{14}$$

and the total amplitude is $\mathcal{M} = \mathcal{M}^{\mathrm{IBA}} + \mathcal{M}^{\mathrm{DM}}$.

Note that EW corrections in IBA become numerically sizable for the cross section at high energies, well above the Z-boson peak. At the lower energies, if the precision required is within a few percent, one can use amplitudes in which the EW form-factors $Z_{\tau q}(s,t)$, $K_q(s,t)$, $K_\tau(s,t)$, $K_{\tau q}(s,t)$ as well as $\Gamma_{vp}(s)$ and $V_{\tau q}(s,t)$ are equal to 1, and the couplings $v_\tau, v_q, a_\tau, a_q, \alpha$ are the *effective* ones of the Z-pole (PDG values [25]). See also the discussion in Appendix A. However, due to the complicated structure of the transverse spin correlations, it might no longer be the case that the BA amplitude is sufficient, see Fig. 3 in Section 4.

In the following, to simplify formulas, we will not indicate explicitly (s,t)-dependence of $v_q(s,t)$, $v_\tau(s,t)$, $Z_{\tau q}(s,t)$, and $V_{\tau q}(s,t)$.

2.2. Spin-correlation matrix R_{ij}

The complete matrix element in the IBA, $\mathcal{M} = \mathcal{M}^{\mathrm{IBA}} + \mathcal{M}^{\mathrm{DM}}$, has been used to derive, with the Mathematica package, Fortran code for the elements R_{ij} of the spin-correlation matrix. Here, we would like to recall explicit analytical form for a few selected elements R_{ij} of particular interest.

The elements R_{ij} are explicitly given in Ref. [12] in the BA and include anomalous dipole moments. Here we elaborate on using $\mathcal{M}^{\mathrm{IBA}}$ (SM with EW corrections) for selected R_{ij} components. In the considered kinematics around the Z-boson pole, it is sufficient to take the limit for the Lorentz factor $\gamma = E_\tau/m_\tau = \sqrt{s}/2m_\tau \gg 1$ and the τ velocity $\beta \approx 1$. We also introduce the modulo squared Z-boson propagator: $D_Z(s) = |d(s)|^2 = (s - M_Z^2)^2 + s^2\Gamma_Z^2/M_Z^2$.

In the formulas for R_{ij} below, we explicitly assume that a_q, a_τ are real, while v_q, v_τ can be complex. For the transverse–transverse (TT) (1–1), transverse–normal (TN) (1–2), and normal–normal (NN) (2–2) spin-correlation elements, we obtain

$$R_{11}^{(\gamma),\mathrm{IBA}} = \frac{e^4}{4}\, Q_q^2 Q_\tau^2\, |V_{\tau q}|^2 \sin^2\theta\,,$$

$$R_{11}^{(Z),\mathrm{IBA}} = \frac{e^4\, s^2}{64 s_{\mathrm{W}}^4 c_{\mathrm{W}}^4 D_Z(s)} |Z_{\tau q}|^2 \left(a_q^2 + |v_q|^2\right) \left(|v_\tau|^2 - a_\tau^2\right) \sin^2\theta\,,$$

$$R_{11}^{(Z\gamma),\mathrm{IBA}} = \frac{e^4\, s}{8 s_{\mathrm{W}}^2 c_{\mathrm{W}}^2 D_Z(s)}\, Q_q Q_\tau$$

$$\times \left[\left(s - M_Z^2\right) \mathrm{Re}\left(v_\tau v_q\, V_{\tau q}^*\, Z_{\tau q}\right) + s\frac{\Gamma_Z}{M_Z} \mathrm{Im}\left(v_\tau v_q\, V_{\tau q}^*\, Z_{\tau q}\right)\right] \sin^2\theta\,, \quad (15)$$

$$R_{12}^{(\gamma),\mathrm{IBA}} = 0\,,$$

$$R_{12}^{(Z),\mathrm{IBA}} = -\frac{e^4\, s^2}{32 s_{\mathrm{W}}^4 c_{\mathrm{W}}^4 D_Z(s)} |Z_{\tau q}|^2 \left(a_q^2 + |v_q|^2\right)\, a_\tau\, \mathrm{Im}(v_\tau) \sin^2\theta\,,$$

$$R_{12}^{(Z\gamma),\mathrm{IBA}} = \frac{e^4\, s}{8 s_{\mathrm{W}}^2 c_{\mathrm{W}}^2 D_Z(s)}\, Q_q\, Q_\tau$$

$$\times a_\tau \left[\left(s - M_Z^2\right) \mathrm{Im}\left(v_q\, V_{\tau q}^*\, Z_{\tau q}\right) - s\frac{\Gamma_Z}{M_Z} \mathrm{Re}\left(v_q\, V_{\tau q}^*\, Z_{\tau q}\right)\right] \sin^2\theta\,. \quad (16)$$

For the longitudinal polarisation elements, one finds

$$R_{34}^{(\gamma),\mathrm{IBA}} = 0\,,$$

$$R_{34}^{(Z),\mathrm{IBA}} = -\frac{e^4\, s^2}{32 s_{\mathrm{W}}^4 c_{\mathrm{W}}^4 D_Z(s)} |Z_{\tau q}|^2$$

$$\times \left[a_\tau \left(a_q^2 + |v_q|^2\right) \mathrm{Re}(v_\tau) \left(1 + \cos^2\theta\right) + 2 a_q \left(a_\tau^2 + |v_\tau|^2\right) \mathrm{Re}(v_q) \cos\theta\right],$$

$$R_{34}^{(Z\gamma),\mathrm{IBA}} = -\frac{e^4\, s}{8 s_{\mathrm{W}}^2 c_{\mathrm{W}}^2 D_Z(s)}\, Q_q Q_\tau$$

$$\times \left\{a_\tau \left[\left(s - M_Z^2\right) \mathrm{Re}(v_q\, V_{\tau q}^*\, Z_{\tau q}) + s\frac{\Gamma_Z}{M_Z} \mathrm{Im}(v_q\, V_{\tau q}^*\, Z_{\tau q})\right] \left(1 + \cos^2\theta\right)\right.$$

$$\left. + 2 a_q \left[\left(s - M_Z^2\right) \mathrm{Re}\left(v_\tau\, V_{\tau q}^*\, Z_{\tau q}\right) + s\frac{\Gamma_Z}{M_Z} \mathrm{Im}(v_\tau\, V_{\tau q}^*\, Z_{\tau q})\right] \cos\theta\right\}. \quad (17)$$

Finally, the elements R_{44} are

$$
\begin{aligned}
R_{44}^{(\gamma),\mathrm{IBA}} &= \frac{e^4}{4} Q_q^2 Q_\tau^2 |V_{\tau q}|^2 \left(1+\cos^2\theta\right) , \\
R_{44}^{(Z),\mathrm{IBA}} &= \frac{e^4\, s^2}{64 s_{\mathrm{W}}^4 c_{\mathrm{W}}^4 D_Z(s)} |Z_{\tau q}|^2 \\
&\times \Big[\left(a_q^2+|v_q|^2\right)\left(a_\tau^2+|v_\tau|^2\right)\left(1+\cos^2\theta\right) + 8\, a_q a_\tau \mathrm{Re}(v_q)\,\mathrm{Re}(v_\tau)\cos\theta \Big] , \\
R_{44}^{(Z\gamma),\mathrm{IBA}} &= \frac{e^4\, s}{8 s_{\mathrm{W}}^2 c_{\mathrm{W}}^2 D_Z(s)} Q_q Q_\tau \\
&\times \Big\{ \Big[\left(s-M_Z^2\right) \mathrm{Re}\left(V_{\tau q}^*\, Z_{\tau q}\, v_q v_\tau\right) + s\frac{\Gamma_Z}{M_Z} \mathrm{Im}\left(V_{\tau q}^*\, Z_{\tau q}\, v_q v_\tau\right) \Big] \left(1+\cos^2\theta\right) \\
&+ 2\, a_q a_\tau \Big[\left(s-M_Z^2\right) \mathrm{Re}\left(V_{\tau q}^*\, Z_{\tau q}\right) + s\frac{\Gamma_Z}{M_Z} \mathrm{Im}\left(V_{\tau q}^*\, Z_{\tau q}\right) \Big] \cos\theta \Big\} .
\end{aligned}
\tag{18}
$$

In these equations, θ is the scattering angle of the outgoing τ^- lepton with respect to the quark q.

In the IBA, the following symmetry relations hold near the Z-boson peak:

$$
R_{22}^{\mathrm{IBA}} = -R_{11}^{\mathrm{IBA}} , \qquad R_{21}^{\mathrm{IBA}} = R_{12}^{\mathrm{IBA}} , \qquad R_{43}^{\mathrm{IBA}} = R_{34}^{\mathrm{IBA}} \tag{19}
$$

for the contributions from γ, Z, and $Z\gamma$.

Note that to account for the quark color average, one should include an additional factor of $1/3$ in Eqs. (15)–(18).

Omitting EW corrections means setting $\Gamma_{vp} = 1$, $Z_{\tau q} = K_{\tau q} = K_\tau = K_q = 1$, and $V_{\tau q} = 1$. In this approximation, v_q, v_τ are real and constant, and formally $\mathcal{M}^{\mathrm{IBA}} = \mathcal{M}^{\mathrm{BA}}$, *i.e.* matrix element in the BA. If the *effective* couplings are used in the $\mathcal{M}^{\mathrm{BA}}$ calculation, most of the effects on the cross section and longitudinal polarisation are restored. But not necessarily for TN correlation, which is sensitive to $\mathrm{Im}(v_\tau)$ in the leading term at the Z pole.

2.3. Introducing phase-shift between vector and axial-vector couplings

The measurement of the ALEPH Collaboration [19] of TN and TT spin correlations allowed the authors to quantify limits on the phase-shift between vector and axial-vector $Z\tau\tau$ couplings. Motivated by this measurement, we included in the initialisation of the TauSpinner program an option which allows one to introduce a similar phase-shift.

The structure of $\mathcal{M}^{\mathrm{IBA}}$ discussed in Section 2.1 has been derived with the convention for the EW form-factors being complex, and the lowest-order couplings being real. Staying within this convention, we introduce the phase-shift Φ not directly to the definition of the couplings themselves but as

rescaling of the EW form-factors in the following manner:

$$\begin{aligned} Z_{\tau q} \to Z'_{\tau q} &= Z_{\tau q} \times \mathrm{e}^{-i\Phi}\,, \\ K_{\tau} \to K'_{\tau} &= K_{\tau} \times \mathrm{e}^{i\Phi}\,, \\ K_{\tau q} \to K'_{\tau q} &= K_{\tau q} \times \mathrm{e}^{i\Phi}\,. \end{aligned} \tag{20}$$

Expression (11) of $\mathcal{M}^{\mathrm{IBA}}$ can now be written as

$$\begin{aligned} \mathcal{M}^{\mathrm{IBA}} \;\to\; & \frac{e^2}{s} Q_q Q_\tau \, V_{\tau q}(s,t)\, \gamma_\mu \otimes \gamma^\mu \\ & + \Big(\frac{g_Z}{2}\Big)^2 \frac{Z_{\tau q}(s,t)}{d(s)}\, \mathrm{e}^{-i\Phi}\, \gamma_\mu \left[T_{3q} - 2Q_q s^2_{\mathrm{W}} K_q(s,t) - a_q \gamma_5\right] \\ & \otimes \gamma^\mu \left[T_{3\tau} - 2Q_\tau s^2_{\mathrm{W}} K_\tau(s,t) \mathrm{e}^{i\Phi} - a_\tau \gamma_5\right]\,. \end{aligned} \tag{21}$$

Note that the factor $V_{\tau q}(s,t)$ in Eq. (13) does not change under the transformation (20). There is no need to re-derive expressions for R_{ij} starting from the definition of $\mathcal{M}^{\mathrm{IBA}}$ in (21), instead, we can redefine the vector coupling for the τ lepton as follows:

$$v_\tau \to v'_\tau = T_{3\tau} - 2Q_\tau s^2_{\mathrm{W}} K_\tau(s,t) \mathrm{e}^{i\Phi}\,. \tag{22}$$

Now, we can express elements R_{ij}, detailed in Section 2.2 (Eqs. (15)–(18)), using v'_τ instead of v_τ. Note also that $|Z_{\tau q}(s,t)| = |Z_{\tau q}(s,t)\mathrm{e}^{-i\Phi}|$. Using (22) we can calculate the phase Φ_{v_τ} of the vector coupling, defined via $v'_\tau = |v'_\tau| \mathrm{e}^{i\Phi_{v_\tau}}$, and use equations

$$\begin{aligned} \mathrm{Re}(v'_\tau) &= T_{3\tau} - 2Q_\tau s^2_{\mathrm{W}} \mathrm{Re}(K_\tau(s,t)) \cos(\Phi) + 2Q_\tau s^2_{\mathrm{W}} \mathrm{Im}(K_\tau(s,t)) \sin(\Phi)\,, \\ \mathrm{Im}(v'_\tau) &= -2Q_\tau s^2_{\mathrm{W}} \mathrm{Re}(K_\tau(s,t)) \sin(\Phi) - 2Q_\tau s^2_{\mathrm{W}} \mathrm{Im}(K_\tau(s,t)) \cos(\Phi)\,, \\ |v'_\tau| &= \left[\mathrm{Re}(v'_\tau)^2 + \mathrm{Im}(v'_\tau)^2\right]^{1/2}\,, \end{aligned} \tag{23}$$

and the formulas

$$\sin(\Phi_{v_\tau}) = \mathrm{Im}(v'_\tau)/|v'_\tau|\,, \qquad \cos(\Phi_{v_\tau}) = \mathrm{Re}(v'_\tau)/|v'_\tau|\,. \tag{24}$$

The phase Φ_{v_τ} of the vector coupling comes from the complex form-factor $K_\tau(s,t)$ and the phase-shift Φ imposed with the transformation (20). The relation between Φ and Φ_{v_τ} is not trivial but can be calculated analytically from (23) and (24), and then numerically using tabulated values of $K_\tau(s,t)$.

In the same manner as Eq. (20), one could introduce the phase-shift in the Z-boson couplings to quarks, including the phase Φ into $K_q(s,t)$ instead of $K_\tau(s,t)$

$$\begin{aligned} Z_{\tau q} \to Z'_{\tau q} &= Z_{\tau q} \times \mathrm{e}^{-i\Phi}, \\ K_q \to K'_q &= K_q \times \mathrm{e}^{i\Phi}, \\ K_{\tau q} \to K'_{\tau q} &= K_{\tau q} \times \mathrm{e}^{i\Phi}. \end{aligned} \tag{25}$$

Correspondingly, we can use expressions for R_{ij} starting from the definition of $\mathcal{M}^{\mathrm{IBA}}$ in (21), with the replacement

$$v_q \to v'_q = T_{3q} - 2Q_\tau s^2_{\mathrm{W}} K_q(s,t)\mathrm{e}^{i\Phi}. \tag{26}$$

The rest of the discussion will follow exactly the same path. In this case the TT element R^{IBA}_{11} is not sensitive to the phase-shift, while the TN element R^{IBA}_{12} strongly depends on it (see Section 4).

Let us make an observation that in Eq. (21), the factor $\mathrm{e}^{-i\Phi}$ multiplying $Z_{\tau q}(s,t)$ can be absorbed into the definition of the couplings, leading to the expression for $\mathcal{M}^{\mathrm{IBA}}$

$$\begin{aligned} \mathcal{M}^{\mathrm{IBA}} \;\to\; & \frac{e^2}{s} Q_q Q_\tau \, V_{\tau q}(s,t)\, \gamma_\mu \otimes \gamma^\mu \\ & + \left(\frac{g_Z}{2}\right)^2 \frac{Z_{\tau q}(s,t)}{d(s)}\, \gamma_\mu \left[T_{3q} - 2Q_q s^2_{\mathrm{W}} K_q(s,t) - a_q \gamma_5\right] \\ & \otimes \gamma^\mu \left[T_{3\tau}\mathrm{e}^{-i\Phi} - 2Q_\tau s^2_{\mathrm{W}} K_\tau(s,t) - a_\tau \mathrm{e}^{-i\Phi}\gamma_5\right], \end{aligned} \tag{27}$$

which suggests redefining the axial-vector and vector couplings in the following way:

$$a_\tau \to a''_\tau = a_\tau \mathrm{e}^{-i\Phi}, \qquad v_\tau \to v''_\tau = T_{3\tau}\mathrm{e}^{-i\Phi} - 2Q_\tau s^2_{\mathrm{W}} K_\tau(s,t). \tag{28}$$

Equation (21) and (27) are equivalent and result in the same phase difference between the vector and axial-vector couplings

$$\Phi_{v''_\tau} - \Phi_{a''_\tau} = \Phi_{v'_\tau} - \Phi_{a'_\tau}. \tag{29}$$

As an illustration, in Fig. 1, we present the Φ-dependence of the absolute value of the phase difference $|\Phi_{v'} - \Phi_{a'}|$ for τ lepton, u and d quarks. It was calculated from (23) and (24) for the τ lepton, and (26) for the quarks. In this figure, we set $K_\tau(s,t) = K_q(s,t) = 1.0$ and $s^2_W = 0.23151$. It is seen that the Φ-dependence of $|\Phi_{v'} - \Phi_{a'}|$ for the τ lepton is more pronounced than that for quarks.

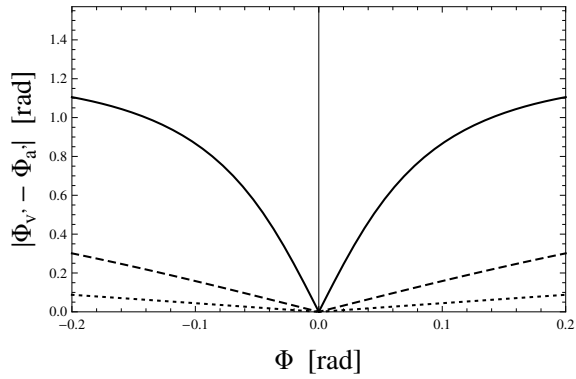

Fig. 1. Relation between the absolute value of the phase difference $|\Phi_{v'} - \Phi_{a'}|$ and the phase-shift Φ of transformation (20) for the τ lepton (solid line) and transformation (25) for the up (dashed line) and down quarks (dotted line).

3. The reweighting algorithm for TauSpinner

3.1. Adjusting convention of $|\mathcal{M}|^2$ calculations and TauSpinner

One can further rearrange Eqs. (9), (10) and introduce normalised elements $r_{ij} = R_{ij}/R_{44}$, factorising out explicitly the spin correlation component of the total cross section, as shown below

$$\frac{\mathrm{d}\sigma}{\mathrm{d}\Omega}\left(\bar{q}q \to \tau^-\tau^+\right) = \frac{\beta}{64\pi^2 s} R_{44}\left(r_{tt} + \sum_{i,j=1}^{3} r_{ij}\, s_i^- s_j^+\right), \qquad r_{tt} = 1\,, \quad (30)$$

where $\beta = (1 - 4m_\tau^2/s)^{1/2}$.

Let us stress that the frame and sign convention of R_{ij} presented in [12] and formulas Eqs. (15)–(18) differ from the ones used in the TauSpinner program, when contracted with the τ leptons polarimetric vectors (recall Eq. (10)). The change in convention which is performed internally in the code reads as follows:

$$\begin{aligned}
R_{tt} &\leftarrow R_{44}\,, & R_{tx} &\leftarrow -R_{42}\,, & R_{ty} &\leftarrow -R_{41}\,, & R_{tz} &\leftarrow -R_{43}\,,\\
R_{xt} &\leftarrow -R_{24}\,, & R_{xx} &\leftarrow R_{22}\,, & R_{xy} &\leftarrow R_{21}\,, & R_{xz} &\leftarrow R_{23}\,,\\
R_{yt} &\leftarrow -R_{14}\,, & R_{yx} &\leftarrow R_{12}\,, & R_{yy} &\leftarrow R_{11}\,, & R_{yz} &\leftarrow R_{13}\,,\\
R_{zt} &\leftarrow -R_{34}\,, & R_{zx} &\leftarrow R_{32}\,, & R_{zy} &\leftarrow R_{31}\,, & R_{zz} &\leftarrow R_{33}\,. \quad (31)
\end{aligned}$$

There are several reasons for the frame orientation differences used in the TauSpinner and Tauola decay library [26] as well. Historical one; in the past, reactions were organized with the z-axis along the e^+ or antiquark direction, whereas now, many authors prefer to use the z-axis along the e^-

or quark direction. This past choice was used for KKMC [27] and Tauola [26] programs. To adjust this, it requires π angle rotation around an axis usually perpendicular to the reaction plane. There is also an overall sign that is affecting τ^+ spin indices of the spin-correlation matrices. This is moved in all Tauola/TauSpinner interfaces [28] from τ decay to spin-correlation matrices. Also, for many of past calculations on which we rely for reference, rest frames of $\tau^\pm$ were chosen to have the common z-axis direction, parallel to the z-axis of the reaction frame (where incoming partons do not define the z direction). For calculations involving NP, we have found that for present-day authors, it is often convenient to allow for distinct frame orientations than that. The easiest way to solve this different convention was to provide for the TauSpinner implementation an adjustment internal routine.

There is also another adjustment, this time for the τ^+ polarimetric vector orientation, as well as its overall sign. At present, this adjustment is shifted into R_{ij} matrix redefinition too[2], even though it does not correspond to a change of its orientation, but is for τ^+ polarimetric vector. Finally,

$$\begin{aligned}
R_{tt} &= R_{44}\,, & R_{tx} &= -R_{42}\,, & R_{ty} &= -R_{41}\,, & R_{tz} &= -R_{43}\,,\\
R_{xt} &= -R_{24}\,, & R_{xx} &= R_{22}\,, & R_{xy} &= R_{21}\,, & R_{xz} &= R_{23}\,,\\
R_{yt} &= R_{14}\,, & R_{yx} &= -R_{12}\,, & R_{yy} &= -R_{11}\,, & R_{yz} &= -R_{13}\,,\\
R_{zt} &= -R_{34}\,, & R_{zx} &= R_{32}\,, & R_{zy} &= R_{31}\,, & R_{zz} &= R_{33}\,.
\end{aligned} \tag{32}$$

With this transformation[3], expressions for the R_{ij} elements of Eq. (32) with $i, j = t, x, y, z$ are used the in TauSpinner event reweighting algorithm discussed in Section 3 for calculating the weight implemented in the TauSpinner code and in Section 4 for presenting numerical results.

The basic formalism of TauSpinner is documented in Ref. [5], Section 2.2, Eqs. (7) to (12). We do not repeat details of this formalism here, nor details how kinematics of the hard process is deciphered from the kinematics of the τ-decay products. We recall, however, a few basic equations for calculating final weights, which allow us to take into account changes in the cross section and spin correlations in the SM and SM+NP models.

The basic equation in the calculation of the cross section is

$$\begin{aligned}
\mathrm{d}\sigma \;=& \sum_{\text{flav}} \int \mathrm{d}x_1\,\mathrm{d}x_2\, f(x_1,...)\, f(x_2,...)\, \mathrm{d}\Omega^{\text{parton level}}_{\text{prod}}\, \mathrm{d}\Omega_{\tau^+}\, \mathrm{d}\Omega_{\tau^-} \\
&\times \left(\sum_{\lambda_1,\lambda_2} |\mathcal{M}^{\text{prod}}_{\text{parton level}}|^2 \right) \left(\sum_{\lambda_1} |\mathcal{M}^{\tau^+}|^2 \right) \left(\sum_{\lambda_2} |\mathcal{M}^{\tau^-}|^2 \right) wt_{\text{spin}}\,,
\end{aligned} \tag{33}$$

[2] It is done separately, in a different place in the code, just before the event weight calculation.

[3] That means that TT, NN, and TN correspond, respectively, to R_{yy}, R_{xx}, and $-R_{yx}$.

where x_1, x_2 denote fractions of the beam momenta carried by the partons, $f(x_1,\ldots)$, $f(x_2,\ldots)$ denote parton density functions (PDFs) of the beams[4], and $\mathrm{d}\Omega$ denote phase-space integration elements, respectively, for the $2\to 2$ hard process and τ decays. Equation (33) represents the product of distributions for the $\tau^{\pm}$ production and decay: $\left(\sum_{\lambda_{1,2}}|\mathcal{M}^{\tau^{\pm}}|^2\right)$ stands for the decay matrix element squared, and $\left(\sum_{\lambda_1,\lambda_2}|\mathcal{M}^{\mathrm{prod}}_{\mathrm{parton\ level}}|^2\right)$ for the production matrix element squared. Only the spin weight wt_{spin} needs input both from the $\tau^{\pm}$ production and decay.

The elements R_{ij} used in the calculation of components of Eq. (33) are taken as a weighted average (with PDFs and production matrix elements squared) over all flavour configurations, as in the following equation:

$$R_{ij}\to\frac{\sum_{\mathrm{flav}}f(x_1,\ldots)f(x_2,\ldots)\left(\sum_{\lambda_1,\lambda_2}|\mathcal{M}^{\mathrm{prod}}_{\mathrm{parton\ level}}|^2\right)R_{ij}}{\sum_{\mathrm{flav}}f(x_1,\ldots)f(x_2,\ldots)\left(\sum_{\lambda_1,\lambda_2}|\mathcal{M}^{\mathrm{prod}}_{\mathrm{parton\ level}}|^2\right)}\,. \tag{34}$$

No new approximation is introduced in this way, the denominator of Eq. (34) cancels explicitly the corresponding factor of Eq. (33).

For the wt_{spin} calculation, the normalised elements $r_{ij}=R_{ij}/R_{tt}$ are used, following Eq. (30)

$$wt_{\mathrm{spin}}=\sum_{i,j=t,x,y,z}r_{ij}h^i_{\tau^+}h^j_{\tau^-}\,. \tag{35}$$

Here, $h^i_{\tau^+}$, $h^j_{\tau^-}$ stand for decay-mode dependent τ polarimetric vectors. Note that wt_{spin} is independent of the PDFs, except through the already averaged over partons contribution from elements r_{ij} of the spin correlations matrix.

To introduce the corrections due to different spin effects and the modified production process in the generated sample (*i.e.* without re-generation of events), one can define the weight wt, representing the ratio of the new-to-old cross sections at each point in the phase space.

Equation (33) for the modified cross section takes then the form

$$\mathrm{d}\sigma_{\mathrm{new}}=\mathrm{d}\sigma_{\mathrm{old}}\;wt^{\mathrm{new/old}}_{\mathrm{prod}}\;wt^{\mathrm{new/old}}_{\mathrm{spin}}\,, \tag{36}$$

where $\mathrm{d}\sigma_{\mathrm{old}}$ is calculated with Eq. (33), wt_{spin} using Eq. (35), and $wt^{\mathrm{new/old}}_{\mathrm{prod}}$ using Eq. (37)

[4] The TauSpinner algorithm does not use information on the flavour of incoming partons from the event record, allowing for the application of its weight also on experimental data.

$$wt_{\rm prod}^{\rm new/old} = \frac{\sum_{\rm flav} f(x_1,\ldots) f(x_2,\ldots) \left(\sum_{\rm spin} |\mathcal{M}_{\rm part\ lev}^{\rm prod}|^2 \right) \Big|_{\rm new}}{\sum_{\rm flav} f(x_1,\ldots) f(x_2,\ldots) \left(\sum_{\rm spin} |\mathcal{M}_{\rm part\ lev}^{\rm prod}|^2 \right) \Big|_{\rm old}} = \frac{R_{tt}|_{\rm new}}{R_{tt}|_{\rm old}} \,. \tag{37}$$

The present implementation assumes that the generated sample has no spin correlations included, however, it can easily be extended[5] to provide weight calculated as

$$wt_{\rm spin}^{\rm new/old} = \frac{\sum_{i,j=t,x,y,z} r_{ij} h_{\tau^+}^i h_{\tau^-}^j \Big|_{\rm new}}{\sum_{i,j=t,x,y,z} r_{ij} h_{\tau^+}^i h_{\tau^-}^j \Big|_{\rm old}} \,. \tag{38}$$

The TauSpinner program provides both weights, $wt_{\rm spin}$ and $wt_{\rm prod}$, which allows one to modify per-event distributions of the sample generated according to $\mathrm{d}\sigma_{\rm old}$ model. The combined weight should be used as a multiplicative product

$$wt = wt_{\rm prod}^{\rm new/old} \ \times \ wt_{\rm spin}^{\rm new/old} \,, \tag{39}$$

where the first term of the weight represents modification of the matrix elements for production, the second one — of the spin correlations. It is nothing but ratios of spin-averaged amplitudes squared for the whole process; new to old. If the analysis is sensitive to changes in the PDF parametrisations used for sample generation and TauSpinner weights calculations, it should be taken into account in the calculation of $wt_{\rm prod}^{\rm new/old}$ and $wt_{\rm spin}^{\rm new/old}$ in Eq. (39). In case the production process is not modified, $wt_{\rm prod}^{\rm new/old}$ is equal to 1. In the case of the originally generated sample without spin correlations, $wt_{\rm spin}^{\rm new/old}$ alone allows one to introduce the desired spin effects.

3.2. Configurations with high p_T jets

Our matrix elements and test observables discussed later rely on simplified kinematics. This would lead to no ambiguities if only parton-level $2 \to 2$ processes were considered. For the general case, this requires attention. In Ref. [29], the question of separating hard (EW) process was addressed, and it was found that with a proper choice of reference frames, one could get the impact of hadronic jets activity absorbed into the adjustment of reference frames. This is possible due to properties of QED and QCD matrix elements and it was explored in preparation for the measurements

[5] Such a special case is available for $\bar{q}q \to \tau\tau$ processes, where, *e.g.* polarisation but not spin correlations, was included in the generated sample.

of the Z and the $W^{\pm}$ properties with the help of templates techniques [30]. The properties seem to be quite general and originating from the properties of the Lorentz group and its representations.

In present applications, we rely on the transverse degrees of freedom, and underlying our methods, separation out of initial-state hadronic (jets) activity needs to attract attention. Especially if events of high-p_{T} jets are present in the analyzed samples. Then, our two choices [10] of reconstructed $2 \to 2$ effective Born frames, one of the Collins–Soper-type [31] and one of the Mustraal-type [32], tend to lead to the biggest differences. We can use these frames both for event-reweighting and for observable building.

4. Numerical results

Numerical results presented below are based on events generated with PYTHIA 8.3 [6] for the pp collisions at 13 TeV, using the $q\bar{q} \to Z/\gamma^* \to \tau\tau$ matrix element, with the invariant-mass range of $\tau\tau$ pair $m_{\tau\tau} = 65$–150 GeV. The τ decays $\tau^{\pm} \to \rho^{\pm}\nu_{\tau}$ were modeled with the Tauola decay library [26] with no spin correlations in the decaying τ pair. In total, we have about 10^6 events. Then, the correlations were added using weight calculated with the TauSpinner program discussed in Section 3, both for effects from the correlations in the SM (EW corrections included) and in the SM+NP models. In Fig. 2, distributions of the invariant mass $m_{\tau\tau}$ and $\cos\theta$ for the generated sample are shown. Using the weight calculated with TauSpinner, the distributions are shown in the SM with the EW effects included.

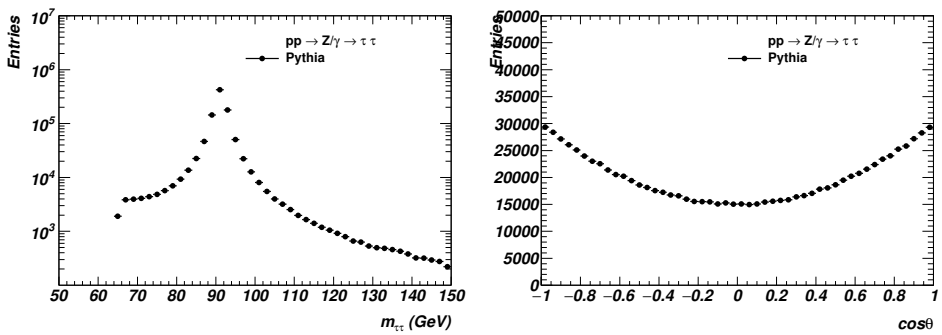

Fig. 2. Distribution of $m_{\tau\tau}$ (left plot) and $\cos\theta$ (right plot) of generated events from the $q\bar{q} \to \tau\tau$ process in pp collisions at a 13 TeV centre-of-mass energy.

In the following, we discuss numerical results for elements of the spin-correlation matrix r_{ij} and identify which component may be most sensitive and provide some evidence of NP. Then, we move to discussing the impact on a few kinematic variables, typically studied in experimental analyses. The

aim is to quantify the effect from spin correlations as present in the SM, and then from NP extensions for $\Phi = \pm 0.1$, $A = 0.1$ or $B = 0.1$ and $X = 0.1$ or $Y = 0.1$. The impact on the integrated cross section due to the introduced NP effects is at the level of a few per mille at the Z-boson pole, and we do not discuss it here, as we are mostly interested in the spin-correlation effects.

4.1. Spin-correlation matrix elements r_{ij}

To simplify the discussion we use as a reference the SM with $\Phi = 0.0$, $A = B = 0$, and $X = Y = 0.0$. In particular, it is assumed that for the application, dipole moments due to QED loop corrections are small and will be dropped out when discussing NP effects. Therefore, for numerical results, we compare the SM predictions with four different settings for NP models

$$(i)\ \Phi = +0.1\,,\ (ii)\ \Phi = -0.1\,,\ (iii)\ X = 0.1\,,\ Y = 0\,,\ (iv)\ X = 0\,,\ Y = 0.1\,. \tag{40}$$

We also studied non-zero values $A = 0.1$ or $B = 0.1$ in the $\gamma\tau\tau$ vertex, but the effect was very small and the corresponding plots are not included here.

The distributions of r_{xx} and r_{xy}, relevant for the transverse spin correlations, are shown in Fig. 3 as functions of $m_{\tau\tau}$. The element r_{xx} is close to 0.5 around the Z peak, decreasing fast below and above. There is almost no difference between IBA and BA. The non-zero element r_{xy} in the BA is due to the $Z\gamma$ interference term only, and is at the level of -0.015 (close to reported value in the case of e^+e^-collisions at LEP [19]), while in the IBA, which includes the EW form-factors, it is at the level of -0.002.

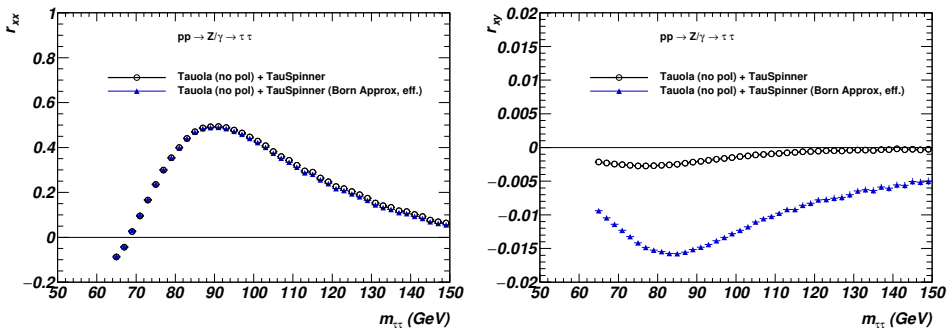

Fig. 3. Distribution of r_{xx} (left plot) and r_{xy} (right plot) as a function of invariant mass $m_{\tau\tau}$. Compared are the SM predictions using $\mathcal{M}^{\mathrm{IBA}}$ (black open circles) and $\mathcal{M}^{\mathrm{BA}}$ with effective couplings (blue triangles).

In Fig. 4, we show similar distributions, but now comparing the SM case in the IBA with the one, where NP effects are introduced as well. The element r_{xx} is almost not sensitive to the phase-shift $\Phi = \pm 0.1$, while r_{xy} shows expected sensitivity, reaching the value of about ± 0.1 for $m_{\tau\tau} = 80$ GeV. The effect of NP model, realized with $X = 0.1$, introduces a sizable increase of r_{yy}. The element r_{xx} also depends on X, however, very weakly and only due to X-dependence of R_{tt}, which enters the definition $r_{xx} = R_{xx}/R_{tt}$, see [12]. This effectively induces a difference between the TT and NN correlation elements r_{yy} and r_{xx}. Finally, as is seen from Fig. 4, the NT correlation element r_{xy} is sensitive to the weak electric form-factor $\mathrm{Re}(Y)$.

Of course, we should note that the values $X = 0.1$, $Y = 0.1$ are a few orders of magnitude larger than the experimental limits on the weak dipole moments obtained in Ref. [23].

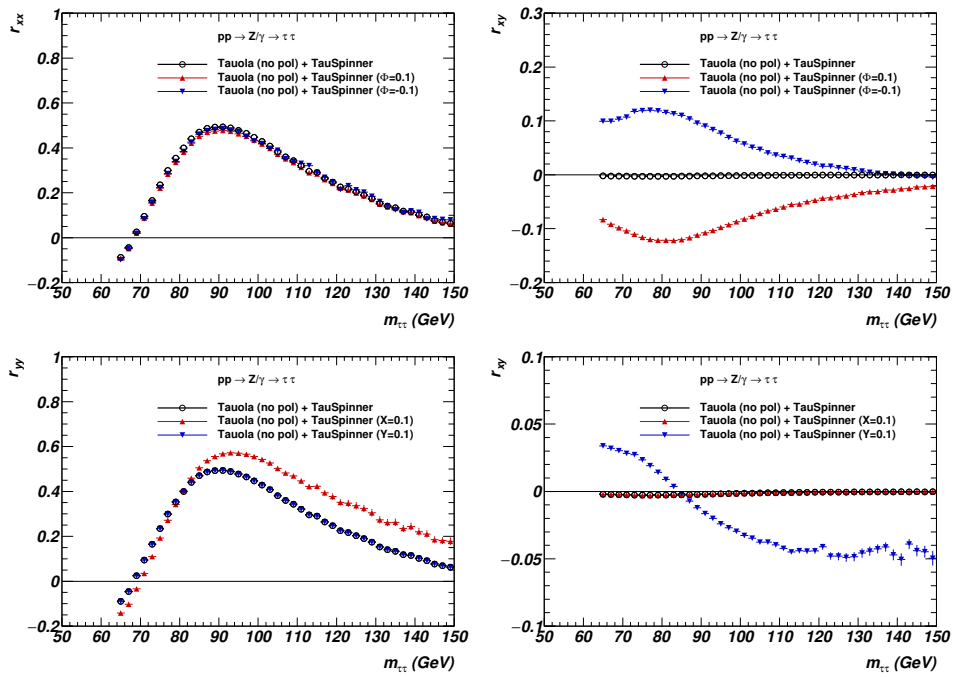

Fig. 4. Distribution of spin-correlation elements r_{xx}, r_{xy}, and r_{yy} as a function of invariant mass $m_{\tau\tau}$. Compared are the SM predictions using $\mathcal{M}^{\mathrm{IBA}}$ (black open circles) and NP ones (red and blue triangles) with $\Phi = \pm 0.1$, $X = 0.1$ or $Y = 0.1$. Left column: r_{xx} (top) and r_{yy} (bottom); right column: r_{xy}.

The distribution of r_{tz}, relevant for the longitudinal polarisation, is shown as a function of $m_{\tau\tau}$ in Fig. 5. The element r_{tz} is almost insensitive to the phase-shift $\Phi = \pm 0.1$, or $Y = 0.1$, while it is sensitive to the weak anomalous magnetic moment $X = 0.1$, leading to a possible effect on the τ-polarisation measurement and the related measurement of $\sin\theta_{\mathrm{W}}$ in the $Z \to \tau\tau$ process.

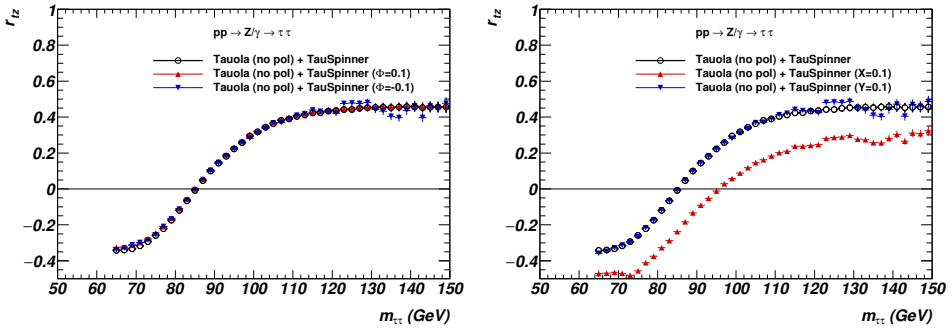

Fig. 5. Distribution of r_{tz} as a function of invariant mass $m_{\tau\tau}$. Compared are the SM predictions using $\mathcal{M}^{\mathrm{IBA}}$ (black open circles) and NP ones (red and blue triangles): $\Phi = \pm 0.1$ (left plot) and $X = 0.1$ or $Y = 0.1$ (right plot).

4.2. Spin effects in $\tau^{\pm} \to \rho^{\pm}\nu_{\tau}$ decay channels

Polarisation and spin correlation effects are illustrated for a few experimentally sensitive kinematical variables listed below:

- ratios E_{ρ}/E_{τ} and $E_{\pi^{\pm}}/E_{\rho}$, which are sensitive to longitudinal polarisation;
- the ratio of the invariant mass of the $\rho^{+}\rho^{-}$ system to that of the $\tau^{+}\tau^{-}$ system, $m_{\rho\rho}/m_{\tau\tau}$, which is sensitive to longitudinal spin correlations;
- two acoplanarity angles calculated from kinematics of decay products of the τ decays: Ψ and ϕ^{*}, which are sensitive to TT and TN spin correlations.

The definition of the Ψ distribution is based on the LEP publications [19, 20]. The direction of the initial quark (beam) is assumed to be along the z-axis in the laboratory frame. The four-vectors of τ-decay products and the beam vector are boosted to the rest frame of the $\rho^{+}\rho^{-}$ system. In this frame, four-vectors are rotated around z- and y-axes such that π^{-} is along the z-axis, and π^{+} lies in the xz-plane. The Ψ angle is defined as an angle between the beam direction and the π^{-} direction.

The definition of the angle ϕ^{*} was proposed for the Higgs CP measurement [33] and was used for the Higgs-boson CP measurement at the LHC [34, 35]. It is calculated as an angle between the planes spanned on

$\pi^{\pm}, \pi^0$ directions for each $\tau^{\pm}$ decay, calculated in the rest frame of the $\rho^+\rho^-$ system. In the case of ϕ^* angle, to preserve sensitivity to the transverse spin correlations, the sample has to be split depending on the angle α_ρ, which is the angle between the beam axis and plane spanned over $\pi^{\pm}, \pi^0$ from one decaying τ lepton, calculated in the laboratory frame (splitting into regions: $\alpha_\rho < \pi/4$ and $\alpha_\rho > \pi/4$).

Both Ψ and ϕ^* distributions show the periodical cosine-shape modulation, once the sample is split into the two sub-samples depending on the sign of the product $y_{\tau^+} \cdot y_{\tau^-}$, where $y_{\tau^\pm} = (E_{\pi^\pm} - E_{\pi^0})/(E_{\pi^\pm} + E_{\pi^0})$. If $y_{\tau^+} \cdot y_{\tau^-} < 0$, we shift $\Psi \to \Psi - \pi/2$ and $\phi^* \to \phi^* - \pi$. This shift was integrated into the definition of Ψ and ϕ^*, respectively, and then the final adjustment is made to respect periodicity, *i.e.* with Ψ being in the range $(-\pi, +\pi)$ and ϕ^* in the range $(0, 2\pi)$. The periodical cosine-like characteristic in the Ψ and ϕ^* distributions is due to non-zero components r_{xx}, r_{yy} of the spin-correlation matrix. However, the phase of it is sensitive to non-diagonal r_{yx} and r_{xy} components.

The distribution of spin correlations sensitive kinematical observables in the SM with $\mathcal{M}^{\rm IBA}$ (black open circles) and NP model with $\Phi = \pm 0.1$ are shown in Fig. 6. Those related to longitudinal polarisation and spin correlations, E_ρ/E_τ, $E_{\pi^\pm}/E_\rho$, and $m_{\rho\rho}/m_{\tau\tau}$, are not affected. The expected small shift in the phase of Ψ and ϕ^* distributions is observed, following an impact on the r_{xy} distribution shown in Fig. 4.

The same set of kinematical distributions, but for NP models with $X = 0.1$ or $Y = 0.1$, is shown in Fig. 7. Distributions of E_ρ/E_τ, $E_{\pi^\pm}/E_\rho$, and $m_{\rho\rho}/m_{\tau\tau}$ show some effect of changed r_{tz} in the case of $X = 0.1$.

One can also observe the effect on Ψ and ϕ^* distributions, either canceling the cosine-like modulation in the Ψ distribution, or changing the phase in the ϕ^* distribution. We expect some effects due to changes in r_{yy} in the case of $X = 0.1$, and in r_{xy} in the case of $Y = 0.1$. However, the interplay between changes in r_{ij} and effects on distributions of sensitive acoplanarity angles seems quite non-trivial[6].

[6] We have presented numerical results with the use of the Collins–Soper frames for the implementation of transverse spin and other effects, EW corrections and NP. We have also used the Mustraal frame for that purpose. It had no impact on the results if the τ-pair transverse momentum was set to zero or was negligibly small. However, some of our observables seemed to be less sensitive to the implemented by TauSpinner effect if the Mustraal frame was used. Since the Mustraal frame is more refined, we can expect similar sensitivity when actual data are used. Alternatively, an optimization of observables should be performed. Unfortunately, this requires major effort, possibly taking into account detector response and detection smearing, so we are bound to leave the topic for future work.

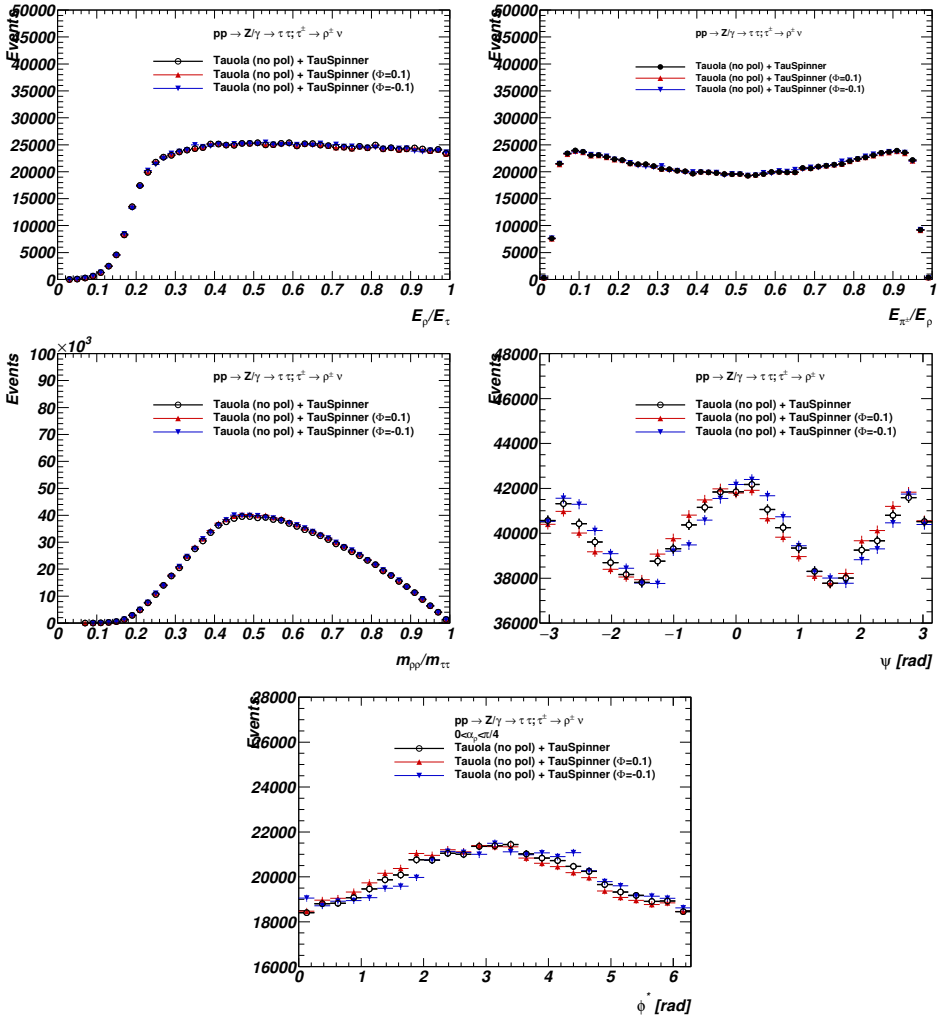

Fig. 6. Distribution of spin correlations sensitive kinematical observables. Compared are the SM predictions $\mathcal{M}^{\mathrm{IBA}}$ (black open circles) and NP ones (red and blue triangles) with $\Phi = \pm 0.1$. Both τ leptons decay via $\tau^{\pm} \to \rho^{\pm}\nu_{\tau} \to \pi^{\pm}\pi^{0}\nu_{\tau}$.

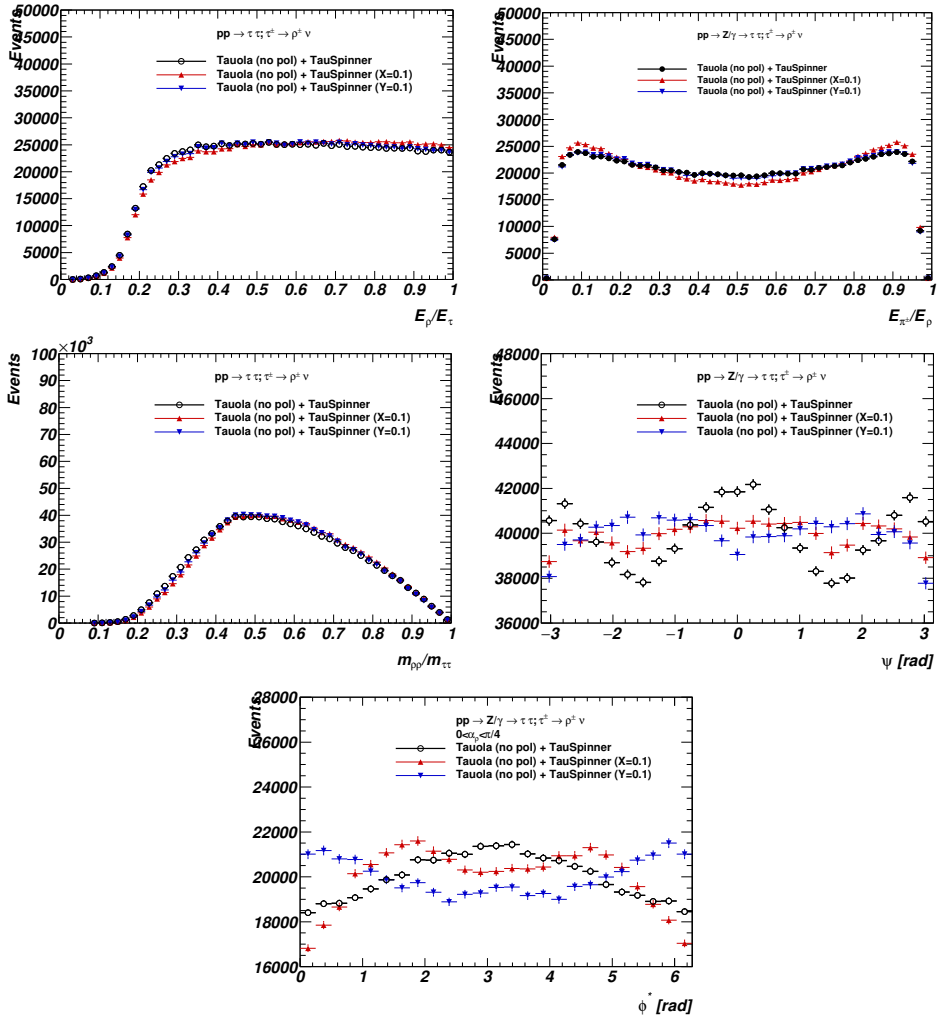

Fig. 7. Distribution of spin correlations sensitive kinematical observables. Compared are the SM predictions $\mathcal{M}^{\rm IBA}$ (black open circles) and NP ones (red and blue triangles) with $X = 0.1$, or $Y = 0.1$. Both τ leptons decay via $\tau^{\pm} \to \rho^{\pm}\nu_{\tau} \to \pi^{\pm}\pi^{0}\nu_{\tau}$.

5. Summary and outlook

We have reviewed the dominant components of spin correlation matrices in $pp \to \tau\tau$ production with subsequent τ decays. For that purpose, matrix element calculation was performed, including generic form-factors of potential New Physics. Already, the SM interactions in the Born Approximation feature vector and axial-vector couplings, distinct for incoming partons and outgoing τ leptons. The picture complicates further in the Improved Born Approximation due to the electroweak corrections which effectively introduce additional phases to the couplings, on top of the phase of the Z-boson propagator with respect to the propagator of the γ exchange. This requires attention as it may be expected to mimic effects of New Physics signature. That is why, not only New Physics effects were installed into the TauSpinner event re-weighting algorithm, but it was assured that they can be studied simultaneously with the electroweak corrections.

After describing formalism, the discussion on the numerical predictions for selected terms of the spin-correlation matrix was presented. The focus was on the transverse spin correlations, which usually are not so often discussed in the literature, in particular for pp collisions.

Several sensitive distributions were studied, first for elements of the spin correlation matrix, later for some semi-realistic distributions in which τ leptons decay into the channels $\tau^+ \to \rho^+\bar{\nu}_\tau \to \pi^+\pi^0\bar{\nu}_\tau$, $\tau^- \to \rho^-\nu_\tau \to \pi^-\pi^0\nu_\tau$. It was shown that exploring spin correlation can improve sensitivity of experiments to New Physics effects. On the other hand, if spin correlations are not taken into account, experimental selection may bias measurements of cross sections and even mimic the presence of New Physics.

This project was supported in part by funds of the National Science Centre (NCN), Poland, grant No. 2023/50/A/ST2/00224 and of COPIN-IN2P3 Collaboration with LAPP-Annecy. A.Yu.K. is grateful to the M. Smoluchowski Institute of Physics of the Jagiellonian University and the Institute of Nuclear Physics Polish Academy of Sciences for support. The majority of the numerical calculations were performed at the PLGrid Infrastructure of the Academic Computer Centre CYFRONET AGH in Kraków, Poland.

Appendix A

Transverse spin correlations at Z-boson pole

As a follow-up from the discussion in Section 2.3, we can proceed with finding the correspondence of R_{ij}, discussed here, and transverse–transverse (TT) and transverse–normal (TN) spin correlations, discussed in Ref. [19]. Let us quote equation (1) for the cross section used in [19]

$$\frac{\mathrm{d}\sigma(s_{\tau^-}, s_{\tau^+})}{\mathrm{d}\Omega_{\tau^-}} = \frac{1}{4s}|P(s)|^2\Big[\, C_0\left(1+\cos^2\theta\right) + 2C_1\cos\theta$$
$$-D_0\left(s^{\mathrm{L}}_{\tau^-} - s^{\mathrm{L}}_{\tau^+}\right)\left(1+\cos^2\theta\right) - 2D_1\left(s^{\mathrm{L}}_{\tau^-} - s^{\mathrm{L}}_{\tau^+}\right)\cos\theta$$
$$-C_0\left(s^{\mathrm{L}}_{\tau^-}s^{\mathrm{L}}_{\tau^+}\right)\left(1+\cos^2\theta\right) - 2C_1\left(s^{\mathrm{L}}_{\tau^-}s^{\mathrm{L}}_{\tau^+}\right)\cos\theta$$
$$+C_2\left(s^{\mathrm{N}}_{\tau^-}s^{\mathrm{N}}_{\tau^+} - s^{\mathrm{T}}_{\tau^-}s^{\mathrm{T}}_{\tau^+}\right)\sin^2\theta + D_2\left(s^{\mathrm{N}}_{\tau^-}s^{\mathrm{T}}_{\tau^+} + s^{\mathrm{T}}_{\tau^-}s^{\mathrm{N}}_{\tau^+}\right)\sin^2\theta\Big]\,, \quad \text{(A.1)}$$

where $P(s)$ is defined in [19], and coefficients C_i, D_i $(i = 0, 1, 2)$ are expressed through the couplings. The first line represents cross section without τ spin, the second line carries information about longitudinal polarisation of τ, the third line — about longitudinal spin correlations, and the last one — about transverse spin correlations. The measured TT and TN spin correlations are defined by the ratios $C_{\mathrm{TT}} = C_2/C_0$ and $C_{\mathrm{TN}} = D_2/C_0$, respectively.

In the notations of our paper, these correlations are related to the elements R_{12}, R_{21}, R_{11}, and R_{22} discussed in Subsection 2.2. For the clarity of the discussion, we consider the IBA and keep only the Z-boson contribution to R^{IBA}_{ij} at the Z pole ($s = M_Z^2$). For the TN correlations, we find (label "IBA" is omitted below)

$$R^{(Z)}_{12} = -2\mathcal{N}|Z_{\tau q}|^2\left(a_q^2 + |v_q|^2\right)a_\tau|v'_\tau|\sin\left(\Phi_{v_\tau}\right)\sin^2\theta\,, \quad \mathcal{N} \equiv \frac{e^4 M_Z^2}{64 s_{\mathrm{W}}^4 c_{\mathrm{W}}^4 \Gamma_Z^2}\,, \quad \text{(A.2)}$$

where Φ_{v_τ} stands for the phase of the $Z\tau\tau$ vector coupling, and the axial-vector coupling remains real and unchanged.

Correspondingly, for the element $R^{(Z)}_{44}$, we have

$$R^{(Z)}_{44} = \mathcal{N}|Z_{\tau q}|^2\Big[\left(a_q^2 + |v_q|^2\right)\left(a_\tau^2 + |v'_\tau|^2\right)\left(1+\cos^2\theta\right)$$
$$+8a_q a_\tau \mathrm{Re}(v_q)|v'_\tau|\cos\left(\Phi_{v_\tau}\right)\cos\theta\Big]\,. \quad \text{(A.3)}$$

Comparing these equations with Eq. (A.1), we obtain the coefficient D_2 of the TN spin correlations

$$D_2 = -2\mathcal{N}|Z_{\tau q}|^2\left(a_q^2 + |v_q|^2\right)a_\tau|v'_\tau|\sin(\Phi_{v_\tau})\,, \quad \text{(A.4)}$$

and the coefficient C_0

$$C_0 = \mathcal{N}|Z_{\tau q}|^2\left(a_q^2 + |v_q|^2\right)\left(a_\tau^2 + |v'_\tau|^2\right) \quad \text{(A.5)}$$

which allows one to calculate $C_{\mathrm{TN}} = D_2/C_0$. Note that our element $r^{(Z)}_{12} = R^{(Z)}_{12}/R^{(Z)}_{44}$ does not coincide with C_{TN} due to the angular factors included in the definition of $R^{(Z)}_{12}$ and $R^{(Z)}_{44}$ (see Eqs. (A.2) and (A.3)).

For the TT spin correlations, we find

$$R_{11}^{(Z)} = \mathcal{N}|Z_{\tau q}|^2 \left(a_q^2 + |v_q|^2\right) \left(|v'_\tau|^2 - a_\tau^2\right) \sin^2\theta\,, \tag{A.6}$$

therefore, the expression corresponding to coefficient C_2, defined in Eq. (A.1), reads as

$$C_2 = \mathcal{N}|Z_{\tau q}|^2 \left(a_q^2 + |v_q|^2\right) \left(a_\tau^2 - |v'_\tau|^2\right) \tag{A.7}$$

which allows one to calculate $C_{\rm TT} = C_2/C_0$. Similarly, the element $r_{11}^{(Z)} = R_{11}^{(Z)}/R_{44}^{(Z)}$ is not equal to $-C_{\rm TT}$ due to the presence of angular factors in $R_{11}^{(Z)}$ and $R_{44}^{(Z)}$ (Eqs. (A.6) and (A.3)).

The denominators in $C_{\rm TN} = D_2/C_0$ and $C_{\rm TT} = C_2/C_0$ cancel out when calculating their ratio, and the expression for TN/TT correlations can be written as

$$\frac{C_{\rm TN}}{C_{\rm TT}} = \frac{D_2}{C_2} = -\frac{R_{12}^{(Z)}}{R_{11}^{(Z)}} = -\frac{2a_\tau|v'_\tau|}{(a_\tau^2 - |v'_\tau|^2)} \sin(\Phi_{v_\tau}) = -\frac{2|a_\tau||v'_\tau|}{(a_\tau^2 - |v'_\tau|^2)} \sin(\Phi_{v_\tau} - \Phi_{a_\tau})\,, \tag{A.8}$$

where the last equality follows from the fact that a_τ is negative and its phase Φ_{a_τ} is equal to π.

The explicit relation between $\sin(\Phi_{v_\tau})$ and phase-shift Φ can be calculated from Eqs. (23) and (24). With all EW form-factors set to 1.0, effectively going from IBA to BA as used in Ref. [19], the coupling v'_τ receives phase only due to the implicit phase-shift and

$$\begin{aligned} \sin(\Phi_{v_\tau}) &= \frac{4s_{\rm W}^2 \sin(\Phi)}{\left(1 - 8s_{\rm W}^2\cos(\Phi) + 16s_{\rm W}^4\right)^{1/2}}\,, \\ \cos(\Phi_{v_\tau}) &= \frac{4s_{\rm W}^2 \cos(\Phi) - 1}{\left(1 - 8s_{\rm W}^2\cos(\Phi) + 16s_{\rm W}^4\right)^{1/2}}\,. \end{aligned} \tag{A.9}$$

With EW corrections restored, which introduce additional phase to the vector coupling, Eqs. (A.9) become more involved and tedious, however, they can be obtained directly from Eqs. (23) and (24).

A more general definition of the TT and TN spin correlations in a wider range of the invariant mass of the τ pair, including EW corrections, γ exchange, and $Z\gamma$ interference, can be obtained following formulas for R_{ij} given in Subsection 2.2. It can also be expanded to include the τ dipole moments, using expressions from [12]. The present implementation in TauSpinner allows one to include those extensions, see Appendix B.

Appendix B

TauSpinner: technical details

The most up-to-date documentation of the TauSpinner algorithms can be found in [5], however, over the years, new developments have been added, as outlined in Section 1. With each of them usually came a dedicated article describing improvement/extension of the physics aspects covered, followed by an example of numerical results and technical additions for the initialisation and usage [10–12, 17].

To summarise those extensions that have happened since [5]:

- New matrix element for $\bar{q}q \to Z/\gamma^* \to \tau^+\tau^-$, with full control on longitudinal polarisation, longitudinal and transverse spin correlations in the Born and Improved Born Approximation. It is discussed here and in [12].
- Matrix element for the $\gamma\gamma \to \tau^+\tau^-$ process with full control on longitudinal polarisation, longitudinal and transverse spin correlations in the Born Approximation. This implementation is flexible enough to be used also for the PbPb collision [17].
- Extension to include in matrix elements listed above form-factors corresponding to dipole and weak dipole moments, in a flexible enough form that can be used to simulate New Physics effects providing it has the same structure of couplings. For $\gamma\gamma \to \tau^+\tau^-$, the dipole moments are included up to the fourth order, and for the $\bar{q}q \to Z/\gamma^* \to \tau^+\tau^-$ process in the lowest order, but in the matrix element of the Improved Born Approximation.
- Extension to include New Physics effects in form of a phase-shift between axial-vector and vector couplings of the Z boson to τ leptons, as discussed in Subsection 2.3.

While we will not make an attempt to include here a complete *user guide*, we try to summarize technical details relevant to what discussed in this paper.

General comments

The spin weight is calculated by assuming that the $\tau\tau$ final state is a product of either $\bar{q}q$ or $\gamma\gamma$ scattering. The calculations of corresponding R_{ij} elements of the spin correlations matrix are invoked and the proportion with which each of the processes contributed to the sum in Eq. (33) depends on the parametrisation of the structure functions $f(x_1, \ldots)$, $f(x_2, \ldots)$. Those represent probabilities of finding in the colliding beams partons (quark, gluon or photon), carrying momentum fractions x_1, x_2.

In the case of proton–proton beams, probabilities $f(x_1, \ldots)$, $f(x_2, \ldots)$ will be taken from the PDFs library, *e.g.* parametrisations of [36, 37] which include also the photon structure functions. The parametrisation used should be indicated during initialisation. For the PbPb collision, the library parametrising the photon flux is not easily available, the user will be required to set it up by hand, for example the $\gamma\gamma$ contribution to R_{ij} can be taken in a fixed proportion to the summed over flavours $\bar{q}q$ one.

Package distribution

The tarball of the package can be downloaded from the web page

https://tauolapp.web.cern.ch/tauolapp/

The TauSpinner package is distributed in the same tarball as the Tauola package, a library for simulating for τ decays, as they share several components of the code, interfaces, and tests.

The installation script is prepared and is located in the main directory

tauola/install-everything.sh

which is installing both Tauola/TauSpinner but also other packages needed for execution of the code and/or examples: HepMC, LHAPDF, PHOTOS, MCTESTER, PYTHIA. One can comment it out and provide a link to the already existing installation in ones own environment.

The examples of use with a short README can be found in the directory tauola/TauSpinner/examples of the distributed tarball. In particular, the following files provide a good starting point.

```
read_particles_from_TAUOLA.cxx
tau-reweight-test.cxx
```

Initialisation

The user is required to configure both $\bar{q}q$ and $\gamma\gamma$ scattering. In case the $\gamma\gamma$ scattering will overly contribute, details of the configuration used for the $\bar{q}q$ process are not relevant. In case the used PDF library does not provide parametrisation of the photon structure function of the proton, the user is required to set also proportion of the $\gamma\gamma$ process with respect to $\bar{q}q$ one, as used at generation GAMfraci and for the desired NP model GAMfrac2i.

To invoke most advanced matrix element implementation, for both $\bar{q}q$ and $\gamma\gamma$ processes, the flag ifkorch = 1 is mandatory, as it invokes consistent flow of the R_{ij} and final weight calculations. Details of the implementation of corresponding matrix elements was given in [12], with extension to higher-order terms for electromagnetic dipole moments for $\gamma\gamma$ processes presented in [17], and allowing for phase-shift between axial-vector and vector couplings as discussed in Section 2.3.

The flag iqed = 0 switches off SM component $A0$ of the magnetic dipole moment, then the total A, B values can be defined by the user.

When including the $\gamma\gamma$ process, at the initalisation step, the user is required to provide values of the dipole moments used for sample generation $A0i, B0i$, $X0i, Y0i$ and those of the NP model for which weight will be calculated Ai, Bi, Xi, Yi. Re-initialisation can be done on the per-event basis, if needed, and the s-dependence of $A(s), B(s), X(s), Y(s)$ can be handled during events processing.

Few options are available for the configuration of EW corrections, which are invoked with the keyGSW flag. They allow to switch on/off some of the form-factors, calculated with the Dizet library [18], more details can be found in [11]. The form-factors are tabulated in table.up and table.down files. The defaults are: keyGSW = 1 (complete set of EW form-factors); keyGSW = 0 (EW form-factors not used, ME with effective couplings).

The legacy implementation of matrix element for the $\bar{q}q \to Z/\gamma^* \to \tau^+\tau^-$ process, documented in [5], is still available. It is invoked with the ifkorch = 0 flag. The default is the Born Approximation with effective couplings and only longitudinal polarisation and spin correlations included. The Improved Born Approximation, including also transverse spin correlations, is used automatically instead, if two files are available from the run directory: table1-1.txt, table2-2.txt. They contain pretabulated r_{ij}, $i, j = x, y$ values calculated with the SANC program [38], see more in [5]. We have checked that the results for r_{xx}, r_{xy} are consistent between legacy implementation using SANC tables and new implementation using ifkorch =1 and Dizet tables are used now.

Choice of the frame for calculating components of the spin weight is steered with flag FrameType. With choice FrameType=1, the Mustraal frame (NLO like) is used, with FrameType=0 (default) the similar to the Collins–Soper frame is used. The frame type can be initialized by invoking: void setFrameType(int _FrameType).

We expect that in a standard usage, initialisation of parameters will be performed once. However, re-initialisation of the parameters is possible on the event-by-event base. One can change *e.g.* setting of EW corrections or dipole moments and process the same event several times for weight calculation. The ratio of the weights calculated for two sets of parameters can then be used to estimate interesting properties of NP models in the process of analysis.

The below snippet of the initialisation code is shown. The path to necessary includes can be found in

tauola/TauSpinner/examples/tau-reweight-test.cxx

```
// initialisation of main flow of TauSpinner
   double CMSENE = 13000.0; // center of mass system energy
                            // used in PDF calculation. For pp collisions only
   bool Ipp   = true;       // for pp collisions, the only option implemented
                            // but gam gam events from PbPb events can be also
                            // processed, see details later
   int Ipol   = 0; // are input samples polarized?
   int nonSM2 = 1; // are we using nonSM calculations?
   int nonSMN = 0; // If we are using nonSM calculations we may want corrections
                   // to shapes only: y/n  (1/0)
   TauSpinner::initialize_spinner(Ipp, Ipol, nonSM2, nonSMN,  CMSENE);

// NEW: initialisation of the frame used for weights calculation
   setFrameType(1); // 1 for Mustraal, 0 for Collins-Soper

// initialisation for Dizet electroweak tables, here you specify location
// where the tables are present, default: in your run directory
// for more documentation see arXiv:2012.10997, arXiv:1808.08616
   char* mumu="table.mu";
   char* downdown= "table.down";
   char* upup= "table.up";
   int initResult=initTables(mumu,downdown,upup);

// initialisation for EW parameters, Born Approximation with effective couplings
// for more documentation see  arXiv:2012.10997, arXiv:1808.08616
   double SWeff=0.2315200;
   double DeltSQ=0.;
   double DeltV=0.;
   double Gmu=0.00001166389;
   double alfinv=128.86674175;
   int keyGSW=1;
   double AMZi=91.18870000;
   double GAM=2.49520000;
   ExtraEWparamsSet(AMZi, GAM, SWeff, alfinv,DeltSQ, DeltV, Gmu,keyGSW);

// initialisation for the qbar q ->tautau matrix elements
// dipole moments and weak dipole moments are set to 0.0 in the qbar q->tautau ME
// flags relevant here are:
   int ifGSW   = 1;  // use EW form-factors
   int ifkorch = 1;  // global flag to switch on ME calculations of arXiv:2307.03526
   int iqed = 0;     // iqed = 1  (if A0 at SM value to be added)
   initialize_GSW(ifGSW, ifkorch, iqed, 0.0, 0.0, 0.0, 0.0, 0.0, 0.0, 0.0, 0.0);

  //  set multipliers of  (Rxx, Ryy, Rxy, Ryx)
  setZgamMultipliersTR(1., 1., 1., 1. );

  // LEGACY: for using implementation of (Rxx, Ryy, Rxy, Ryx) as in arXiv:1802.05459
  // transverse spin correlations Rxx, Ryy, Rxy, Ryx read in  from tables
  // table1-1.txt, table2-2.txt which should be placed in the run directory.
  initialize_GSW(0, 0, 0, 0.0, 0.0, 0.0, 0.0, 0.0, 0.0, 0.0, 0.0);

  // NEW: for using implementation of (Rxx, Ryy, Rxy, Ryx) as in arXiv:2307.03526
  initialize_GSW(1, 1, 0, 0.0, 0.0, 0.0, 0.0, 0.0, 0.0, 0.0, 0.0); // SM with Improved Born
  initialize_GSW(0, 1, 0, 0.0, 0.0, 0.0, 0.0, 0.0, 0.0, 0.0, 0.0); // SM with Effective Born

  // NEW: for using implementation of (Rxx, Ryy, Rxy, Ryx) as in arXiv:2307.03526
  // adding magnetic and electric dipole moments and weak dipole moments
  // example initialisation, requires flags: ifkorch = 1; nonSM2 = 1;
  double ReA = 0.1;
```

```
double ImA = 0.0;
double ReB = 0.0;
double ImB = 0.0;
double ReX = 0.0;
double ImX = 0.0;
double ReY = 0.0;
double ImY = 0.0;
initialize_GSW(1, 1, 0, ReA, ImA, ReB, ImB, ReX, ImX, ReY, ImY); // with Improved Born

// NEW: form-factors from  Dizet electroweak tables  can be scaled
// here use form-factors as in  Dizet electroweak tables, scaled by 1.0
// select option for EW form-factors
int keyGSW = 1;  //default
initialize_GSW_norm(keyGSW, 1.0, 0.0, 1.0, 0.0, 1.0, 0.0, 1.0, 0.0, 1.0, 0.0, 1.0, 0.0);

// NEW: introduce shift between phase of axial and vector couplings of $Z$ to tau leptons
// use scaling for this purpose, as described in Section 2.3
double fi=0.1;
double c=cos(fi);
double s=sin(fi);
initialize_GSW_norm(keyGSW, c, -s, c, s, 1.0, 0.0, c, s, 1.0, 0.0, 1.0, 0.0);
```

The default setting used, if not overwritten during initialisation, can be found at the very top of the file
tauola/TauSpinner/src/tau_reweight_lib.cxx

Calculation of event weights

The spin correlation matrix R_{ij} (coded in Fortran) is used by the weight calculating method (coded in C++).

The elements of the Rij matrix are calculated by routines dipolqq_ and dipolgamma_ respectively for antiquark–quark and $\gamma\gamma$ processes. They are provided in TAUOLA/TauSpinner/src/initwksw.f file. In addition to calculation, the frame re-orientation is provided in these Fortran interfacing routines (Eq. (32)). Also the change of index convention from Fortran 1,2,3,4 to C++ 0,1,2,3 is introduced. Finally, the minus sign originating from the τ^+ V+A coupling instead of the τ^- V−A coupling is introduced there as well. That also explains the sign change in R_{yy} *versus* publication [12].

The dipolqq_(iqed,E,theta,channel,Amz0,Gamz0,sin2W0,alphaQED,ReA0, ImA0,ReB0,mB0,ReX0,ImX0,ReY0,ImY0, GSWr0,GSWi0,Rij) function has several input parameters and output normalised matrix Rij, *i.e.* $r_{ij} = R_{ij}/R_{tt}$. The E, theta denote, respectively, the energy of the scattering antiquark in the $2 \to 2$ parton level centre-of-mass frame and scattering angle of the outgoing τ lepton with respect to antiquark beam direction, also in this frame. The channel denote type of flavour of incoming partons. The A0, B0 denote anomalous magnetic and electric moments. The X0, Y0 denote weak anomalous magnetic and electric moments. The iqed flag switches OFF/ON contribution to A0 from the Standard Model $A(0)_{\rm SM} = 1.17721(5) \times 10^{-3}$

of the anomalous magnetic dipole moment, as calculated in [39]. The Amz0,Gamz0,sin2W0,alphaQED denotes EW parameters at the Born level in the $\alpha(0)$ scheme, and GSWr0,GSWi0 denote EW form-factors used for the Improved Born Approximation.

The dipolgamma_(iqed,E,theta,A0,B0,Rij) function has several input parameters iqed, E, theta, A0, B0 and output normalised matrix Rij, *i.e.* $r_{ij} = R_{ij}/R_{tt}$. The E, theta denote respectively the energy of the scattering photon in the $2 \to 2$ parton level centre-of-mass frame and scattering angle of the outgoing τ lepton with respect to photon beam direction, also in this frame. The A0, B0 denote anomalous magnetic and electric moments. The iqed flag switches OFF/ON contribution to A0 from the Standard Model $A(0)_{\rm SM} = 1.17721(5) \times 10^{-3}$ of the anomalous magnetic dipole moment [39].

For each event, which is read from the input_file by:

```
int status = readParticlesFromTAUOLA_HepMC(input_file, X, tau, tau2,
             tau_daughters, tau_daughters2);
```

calculation of spin weight $WTspin$ and the corresponding relative change to the cross section $WTprod$, due to the introduced NP models can be invoked.

```
double WTspin = calculateWeightFromParticlesH(X, tau, tau2,
                                               tau_daughters,tau_daughters2);
double WTprod = getWtNonSM();
```

By definition, always an average of spin weight $\langle WTspin \rangle = 1.0$. To quantify the impact on a particular kinematical distribution, including spin correlations for a given (SM+NP) model with respect to one used in generated sample, one should use product $WTspin \cdot WTprod$ when filing histograms. It means that only relative change in the cross section, not the absolute one, can be accessed with the present implementation in TauSpinner.

Accessing internal variables

Several functions (*getters*) are available to access internal variables. In particular for each event, with the methods

```
getZgamParametersTR(Rxx, Ryy, Rxy, Ryx);
getZgamParametersL(Rzx, Rzy, Rzz, Rtx, Rty, Rtz);
```

the set of normalised r_{ij} matrix components can be accessed, which might be of interest for monitoring purposes.

REFERENCES

[1] ATLAS Collaboration (G. Aad *et al.*), «A measurement of $\tau\bar{\tau}$ the high-mass production cross-section at $\sqrt{s} = 13$ TeV with the ATLAS detector and constraints on new particles and couplings», *J. High Energy Phys.* **2025**, 054 (2025), arXiv:2503.19836 [hep-ex].

[2] CMS Collaboration (S. Chatrchyan *et al.*), «Measurement of the inclusive Z cross section via decays to tau pairs in pp collisions at $\sqrt{s} = t$ TeV», *J. High Energy Phys.* **2011**, 117 (2011), arXiv:1104.1617 [hep-ex].

[3] ATLAS Collaboration (G. Aad *et al.*), «Measurement of the $Z \to \tau\tau$ cross section with the ATLAS detector», *Phys. Rev. D* **84**, 112006 (2011), arXiv:1108.2016 [hep-ex].

[4] Z. Czyczula, T. Przedzinski, Z. Was, «TauSpinner program for studies on spin effect in tau production at the LHC», *Eur. Phys. J. C* **72**, 1988 (2012), arXiv:1201.0117 [hep-ph].

[5] T. Przedzinski, E. Richter-Was, Z. Was, «Documentation of TauSpinner algorithms: program for simulating spin effects in τ-lepton production at LHC», *Eur. Phys. J. C* **79**, 91 (2019), arXiv:1802.05459 [hep-ph].

[6] C. Bierlich *et al.*, «A comprehensive guide to the physics and usage of PYTHIA 8.3», *SciPost Phys. Codebases* **2022**, 8 (2022), arXiv:2203.11601 [hep-ph].

[7] Sherpa Collaboration, (E. Bothmann *et al.*), «Event generation with Sherpa 2.2», *SciPost Phys.* **7**, 034 (2019), arXiv:1905.09127 [hep-ph].

[8] J. Kalinowski, W. Kotlarski, E. Richter-Was, Z. Was, «Production of τ lepton pairs with high p_{T} jets at the LHC and the TauSpinner reweighting algorithm», *Eur. Phys. J. C* **76**, 540 (2016), arXiv:1604.00964 [hep-ph].

[9] T. Przędziński, E. Richter-Wąs, Z. Wąs, «TauSpinner: a tool for simulating CP effects in $H \to \tau\tau$ decays at LHC», *Eur. Phys. J. C* **74**, 3177 (2014), arXiv:1406.1647 [hep-ph].

[10] E. Richter-Was, Z. Was, «Documentation of TauSpinner approach for electroweak corrections in LHC $Z \to ll$ observables», *Eur. Phys. J. C* **79**, 480 (2019), arXiv:1808.08616 [hep-ph].

[11] E. Richter-Was, Z. Was, «Adequacy of Effective Born for electroweak effects and TauSpinner algorithms for high energy physics simulated samples», *Eur. Phys. J. Plus* **137**, 95 (2022), arXiv:2012.10997 [hep-ph].

[12] S. Banerjee, A.Y. Korchin, E. Richter-Was, Z. Was, «Electron–positron, parton–parton, and photon–photon production of τ-lepton pairs: Anomalous magnetic and electric dipole moments spin effects», *Phys. Rev. D* **109**, 013002 (2024), arXiv:2307.03526 [hep-ph].

[13] A.Y. Korchin, «Spin Effects in tau-lepton Pair Induced by Anomalous Magnetic and Electric Dipole Moments», *Acta Phys. Pol. B Proc. Suppl. B* **17**, 5-A20 (2024).

[14] L. Beresford, J. Liu, «New physics and tau $g-2$ using LHC heavy ion collisions», *Phys. Rev. D* **102**, 113008 (2020), arXiv:1908.05180 [hep-ph]; *Erratum ibid.* **106**, 039902 (2022).

[15] U. Haisch, L. Schnell, J. Weiss, «LHC tau-pair production constraints on a_τ and d_τ», *SciPost Phys.* **16**, 048 (2024), arXiv:2307.14133 [hep-ph].

[16] L. Beresford, S. Clawson, J. Liu, «Strategy to measure tau $g-2$ via photon fusion in LHC proton collisions», *Phys. Rev. D* **110**, 092016 (2024), arXiv:2403.06336 [hep-ph].

[17] A.Y. Korchin, E. Richter-Was, Z. Was, «TauSpinner Algorithms for Including Spin and New Physics Effects in $\gamma\gamma \to \tau\tau$ Process», *Acta Phys. Pol. B* **56**, 10-A4 (2025), arXiv:2506.15213 [hep-ph].

[18] D.Yu. Bardin *et al.*, «ZFITTER v.6.21: A semi-analytical program for fermion pair production in e^+e^- annihilation», *Comput. Phys. Commun.* **133**, 229 (2001), arXiv:hep-ph/9908433.

[19] ALEPH Collaboration (R. Barate *et al.*), «Measurement of the transverse spin correlations in the decay $Z \to \tau^+\tau^-$», *Phys. Lett. B* **405**, 191 (1997).

[20] DELPHI Collaboration (P. Abreu *et al.*), «Measurement of the transverse spin correlation in $Z \to \tau^+\tau^-$ decays», *Phys. Lett. B* **404**, 194 (1997).

[21] S. Banerjee, A.Y. Korchin, Z. Was, «Spin correlations in τ-lepton pair production due to anomalous magnetic and electric dipole moments», *Phys. Rev. D* **106**, 113010 (2022), arXiv:2209.06047 [hep-ph].

[22] V.B. Berestetskii, E.M. Lifshitz, L.P. Pitaevskii, «Quantum Electrodynamics, Course of Theoretical Physics», *Pergamon Press*, Oxford 1982.

[23] ALEPH Collaboration (A. Heister *et al.*), «Search for anomalous weak dipole moments of the τ lepton», *Eur. Phys. J. C* **30**, 291 (2003), arXiv:hep-ex/0209066.

[24] J. Bernabéu, G.A. González-Sprinberg, M. Tung, J. Vidal, «The tau weak-magnetic dipole moment», *Nucl. Phys. B* **436**, 474 (1995), arXiv:hep-ph/9411289.

[25] Particle Data Group (S. Navas *et al.*), «Review of Particle Physics», *Phys. Rev. D* **110**, 030001 (2024).

[26] S. Jadach, Z. Was, R. Decker, J.H. Kuhn, «The τ decay library TAUOLA, version 2.4», *Comput. Phys. Commun.* **76**, 361 (1993).

[27] A. Arbuzov *et al.*, «The Monte Carlo Program KKMC, for the Lepton or Quark Pair Production at LEP/SLC Energies — Updates of electroweak calculations», *Comput. Phys. Commun.* **260**, 107734 (2021), arXiv:2007.07964 [hep-ph].

[28] N. Davidson *et al.*, «Universal interface of TAUOLA: Technical and physics documentation», *Comput. Phys. Commun.* **183**, 821 (2012), arXiv:1002.0543 [hep-ph].

[29] E. Richter-Was, Z. Was, «Separating electroweak and strong interactions in Drell–Yan processes at LHC: leptons angular distributions and reference frames», *Eur. Phys. J. C* **76**, 473 (2016), arXiv:1605.05450 [hep-ph].

[30] E. Richter-Was, Z. Was, «W production at LHC: lepton angular distributions and reference frames for probing hard QCD», *Eur. Phys. J. C* **77**, 111 (2017), arXiv:1609.02536 [hep-ph].

[31] J.C. Collins, D.E. Soper, «Angular distribution of dileptons in high-energy hadron collisions», *Phys. Rev. D* **16**, 2219 (1977).

[32] F.A. Berends, R. Kleiss, S. Jadach, «Monte Carlo simulation of radiative corrections to the processes $e^+e^- \to \mu^+\mu^-$ and $e^+e^- \to qq$ in the Z_0 region», *Comput. Phys. Commun.* **29**, 185 (1983).

[33] K. Desch, A. Imhof, Z. Wąs, M. Worek, «Probing the nature of the Higgs boson at linear colliders with τ spin correlations; the case of mixed scalar–pseudoscalar couplings», *Phys. Lett. B* **579**, 157 (2004), arXiv:hep-ph/0307331.

[34] ATLAS Collaboration (G. Aad *et al.*), «Measurement of the CP properties of Higgs boson interactions with τ-leptons with the ATLAS detector», *Eur. Phys. J. C* **83**, 563 (2023), arXiv:2212.05833 [hep-ex].

[35] CMS Collaboration (A. Tumasyan *et al.*), «Analysis of the CP structure of the Yukawa coupling between the Higgs boson and τ leptons in proton–proton collisions at $\sqrt{s} = 13$ TeV», *J. High Energy Phys.* **2022**, 012 (2022), arXiv:2110.04836 [hep-ex].

[36] S.R. Klein *et al.*, «STARlight: A Monte Carlo simulation program for ultra-peripheral collisions of relativistic ions», *Comput. Phys. Commun.* **212**, 258 (2017), arXiv:1607.03838 [hep-ph].

[37] CTEQ-TEA Collaboration (K. Xie *et al.*), «Photon PDF within the CT18 global analysis», *Phys. Rev. D* **105**, 054006 (2022), arXiv:2106.10299 [hep-ph].

[38] A. Andonov *et al.*, «Standard SANC modules», *Comput. Phys. Commun.* **181**, 305 (2010), arXiv:0812.4207 [physics.comp-ph].

[39] S. Eidelman, M. Passera, «Theory of the τ Lepton Anomalous Magnetic Moment», *Mod. Phys. Lett. A* **22**, 159 (2007), arXiv:hep-ph/0701260.